Earth-Science Reviews 139 (2014) 59–82

Contents lists available at ScienceDirect

Earth-Science Reviews

journal homepage: www.elsevier.com/locate/earscirev

Proterozoic Fe–Cu metallogeny and supercontinental cycles of the southwestern Yangtze Block, southern China and northern Vietnam

Mei-Fu Zhou [a,b,*], Xin-Fu Zhao [b,c], Wei Terry Chen [a,b], Xiao-Chun Li [b], Wei Wang [b,c], Dan-Ping Yan [d], Hua-Ning Qiu [e]

[a] State Key Laboratory of Ore Deposit Geochemistry, Institute of Geochemistry, Chinese Academy of Sciences, Guiyang 550002, China
[b] Department of Earth Sciences, The University of Hong Kong, Hong Kong SAR, China
[c] Faculty of Earth Resources, China University of Geosciences, Wuhan 430074, China
[d] School of Earth Sciences, China University of Geosciences, Beijing, China
[e] Key Laboratory of Isotope Geochronology and Geochemistry, Guangzhou Institute of Geochemistry, Chinese Academy of Sciences, P.O. Box 1131, Guangzhou 510640, China

ARTICLE INFO

Article history:
Received 28 June 2013
Accepted 22 August 2014
Available online 16 September 2014

Keywords:
Fe–Cu deposits
$^{40}Ar/^{39}Ar$ dating
Kangdian IOCG metallogenic province
Multiple mineralization events
Supercontinents
SW China

ABSTRACT

The Yangtze Block has a Paleoproterozoic and Archean basement and was traditionally thought to have been cratonized after the Neoproterozoic. Recent studies reveal that the southwestern part is remarkably different from other parts of the block. Major Fe–Cu deposits are present in the southwestern part where they form the Kangdian IOCG metallogenic province in southern China and northern Vietnam. Large Fe–Cu deposits include Lala and Xikuangshan to the north, Yinachang in the center, Dahongshan and Sin Quyen to the south and possibly Shilu to the south-east. These deposits are characterized by an association of Fe-oxides and Cu-sulfides with REE, Mo, Co, Ag, and Au as common by-products.

The ore deposits are hosted in variably metamorphosed, late Paleoproterozoic rocks (~1.65–1.7 Ga) of the Dahongshan, Dongchuan, Hekou, Sin Quyen, and Shilu Groups, although the age of the Shilu Group in Hainan is poorly constrained. Molybdenite separates from the Yinachang and the Lala deposits have Re–Os model ages of 1.66 and ~1.0 Ga. These ages suggest that the Fe–Cu deposits formed in multiple mineralization events over an exceptionally broad time range. There was a minor hydrothermal overprint at ~1.45 Ga. Biotite, amphibole, and quartz from several deposits have $^{40}Ar/^{39}Ar$ plateau ages ranging from 850 to 780 Ma, but cluster at 830–820 Ma. These $^{40}Ar/^{39}Ar$ ages are considerably younger than the Fe–Cu deposits and are interpreted as the result of thermal resetting of the K–Ar system during the Neoproterozoic, consistent with the extensive Neoproterozoic igneous activity in the Yangtze Block.

The mineralization styles of the 1.66 Ga deposits in the southwestern Yangtze Block are similar to those of contemporaneous IOCG deposits in other blocks within the Columbia supercontinent, including those in the Leichhardt and Calvert Superbasins, the Mount Isa Inlier, Australia, and those in the Khetri copper belt, NW India. Together with similar hosting strata and associated igneous rocks, the occurrence of these deposits leads us to propose that these blocks were adjacent to each other in the reconstructed Columbia supercontinent. Both South China and India remained together during the assembly of the supercontinent Rodinia and have undergone extensive Neoproterozoic magmatism that overprinted the Fe–Cu deposits.

Contents

* Corresponding author at: Department of Earth Sciences, The University of Hong Kong, Hong Kong SAR, China. Tel.: +852 2857 8252; fax: +852 2517 6912.
E-mail address: zhoumeifu@hotmail.com (M.-F. Zhou).

http://dx.doi.org/10.1016/j.earscirev.2014.08.013
0012-8252/

1. Introduction

A metallogenic province may have undergone multiple tectonothermal events (e.g., Weihed et al., 2005). If such events were related to assembly of paleo-supercontinents or events within amalgamated blocks of such a continent, then deposits in particular regions may be comparable to those in previously adjacent blocks separated by supercontinent breakup. Thus, reconstruction of supercontinental cycles is important for understanding the origin of the deposits and thus useful for mineral exploration (e.g., Cawood and Hawkesworth, 2013).

Proterozoic iron-oxide–copper–gold (IOCG) deposits around the world may have formed through multiple mineralization events, some of which could have been separated by many hundreds of millions of years (e.g. Smith et al., 2009; Chen et al., 2010; Duncan et al., 2011). Zircon U–Pb and molybdenite Re–Os dating have shown that IOCG mineralization in the Cloncurry District of Australia was initiated at ~1.65 Ga, reached its peak at ~1.55 to ~1.49 Ga, and may have continued until ~1.36 Ga as indicated by late carbonate veins (Duncan et al., 2011). The Fe–Cu deposits in the Khetri copper belt of NW India are hosted in Paleoproterozoic strata and are thought to have formed initially at 1.65 Ga, and possibly 850 Ma as well (Knight et al., 2002).

The Yangtze Block has an Archean to Paleoproterozoic basement and was probably cratonized after the Neoproterozoic (e.g. Zhou et al., 2009; Wang et al., 2010; Zhao et al., 2011; Wang et al., 2012a,b). The Precambrian tectonic evolution of the Yangtze Block and its metallogeny in relation to supercontinental cycles are poorly understood. Whether the Yangtze Block was part of the proposed supercontinents, Rodinia and Columbia, and its location in the reconstruction of these two supercontinents have long been matters of debate. Recent studies highlight the dramatic differences between the southwestern and eastern parts of the Yangtze Block (e.g., Zhao et al., 2011; and references therein). Proterozoic Fe–Cu deposits only present in the southwestern Yangtze Block define the Kangdian metallogenic province (Figs. 1 and 2) and are particularly important to understand the link of tectonothermal events and supercontinental cycles.

Many Fe–Cu deposits in the Kangdian region, which extends from southern Sichuan Province, southward through Yunnan Province, and into northern Vietnam (Figs. 1 and 2), have been regarded as typical IOCG deposits (Zhao and Zhou, 2011; Chen and Zhou, 2012). The Sin Quyen deposit in northern Vietnam and the Shilu deposit in Hainan Island of South China have mineralization styles similar to those of other deposits and are considered to represent the southeastern extension of the metallogenic province, which was displaced by the Tertiary Red River fault zone (Figs. 1 and 3). Some of these deposits are world-class and have unique mineralization styles, but only a few published descriptions are available and these are mostly in Chinese. Our recent studies suggest that the IOCG deposits may have formed in multiple tectonothermal events (Zhao and Zhou, 2011; Chen and Zhou, 2012; Zhao et al., 2013). The mineralization styles and ages of these deposits are comparable to those in the North Australian craton and NW India. Thus, it is possible that these IOCG provinces or belts can be linked in supercontinent reconstructions.

In this paper, we review the Precambrian geology of the Yangtze Block and outline the main features of the Kangdian metallogenic province. Two major mineralization events are recognized based on available molybdenite Re–Os isotopic ages for the largest deposits. We also report new $^{40}Ar/^{39}Ar$ ages for biotite and amphibole from several deposits. The new Ar–Ar dates, for the first time, provide precise and reliable constraints on a much younger tectonothermal event that can be linked with the giant Neoproterozoic tectonomagmatic event in the Yangtze Block. Available information about the tectonothermal evolution of the Kangdian IOCG province is used to understand the tectonic setting in which the deposits formed. These deposits are compared with those in NW India and North Australia, and a possible link between Fe–Cu mineralization and Proterozoic supercontinental cycles is further discussed. We propose a potential connection between South China, India, and Australia in the supercontinent Columbia.

2. Geological background

2.1. Regional framework of the Yangtze Block

The Yangtze Block is bounded by the Cathaysia Block to the southeast and by the Tibetan Plateau to the west (Fig. 1), and separated from the Indochina Block to the south by the Song Ma Suture. The Yangtze and Cathaysia Blocks were welded together at ca. 830 Ma (e.g. Zhou et al., 2009; Wang et al., 2010; Zhao et al., 2011; Wang et al., 2012a,b).

The Precambrian basement is predominately exposed in the southwestern, eastern, and northern parts of the Yangtze Block (Fig. 1). Zheng et al. (2006) suggested a wide distribution of Archean rocks in

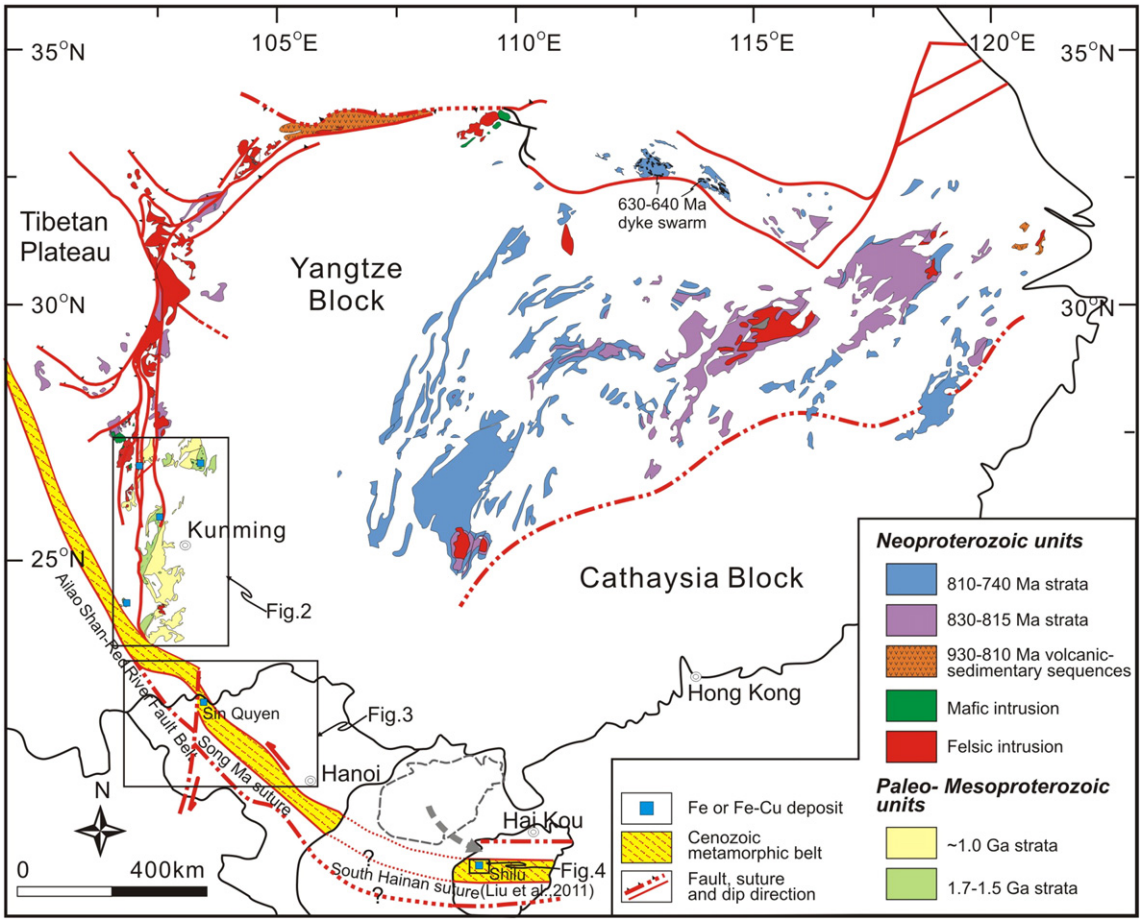

Fig. 1. Simplified geological map of the Yangtze Block, showing the distribution of major Proterozoic strata and Neoproterozoic igneous bodies (modified from Zhou et al., 2008; Liu et al., 2011; Zhao et al., 2011).

the unexposed basement of the Yangtze Block based on U–Pb and Hf isotopic data from zircon xenocrysts in Paleozoic lamproites. The western, northern and southeastern parts of the Yangtze Block have different Precambrian geology (Fig. 1). In the northern part, the Kongling Complex contains igneous and metamorphic rocks as old as 3.3 Ga (Zhang et al., 2006a; Gao et al., 2011), but crystalline basement complexes are not exposed in the other parts of the block.

The eastern part of the Yangtze Block is known as the Jiangnan orogen. Proterozoic strata include the 930–890-Ma Shuangxiwu arc volcanic rocks and the Sibao Group. The Sibao Group and its equivalents, the Fanjingshan, Lengjiaxi, and Shuangqiaoshan Groups, were traditionally thought to be Mesoproterozoic and are actually Neoproterozoic sequences (830–815 Ma) deposited in back-arc basins (Wang et al., 2013). The sedimentary rocks of these groups contain abundant Neoproterozoic detrital zircons (970–830 Ma) (Shu et al., 1993; Li et al., 2009; Wang et al., 2010, 2013). Subsequently, amalgamation between the Yangtze and Cathaysia Blocks occurred as evidenced by the ~824 Ma ophiolitic complex in southern Anhui Province (Zhang et al., 2012b) and by a regional scale unconformity above which the ~800–730 Ma Banxi Group and its equivalents deposited (Zhao et al., 2011). These younger strata are products of large-scale rifting, probably initiated by back-arc extension related to subduction in the western Yangtze Block (Zhao et al., 2011). The cessation of rift-related sedimentation and volcanism was synchronous with the end of subduction in the western Yangtze Block. After that, the entire Yangtze Block became a passive margin with deposition of the 725–630-Ma Cryogenian glacial–interglacial sedimentary sequences.

The Mesozoic–Cenozoic collision between the Indian subcontinent and Eurasia has displaced Indochina at least 500 km southeastwards relative to South China (Tapponnier et al., 1990). This displacement along the Red River fault zone is marked by a ductile metamorphic shear zone (Figs. 1–3). This fault zone extends for more than 1000 km from the Gulf of Tonkin to Tibet. Both the Red River fault zone and the Song Ma suture zone may extend to Hainan Island of South China (Fig. 1). Tertiary spreading of the South China Sea rifted the island away from the South China Block (Fig. 1; Replumaz and Tapponnier, 2003; Z.C. Chen et al., 2013; L. Chen et al., 2013). Two nearly west–east-striking regional faults, the Jiusuo–Lingshui fault on the south and the Wangwu–Wenjiao fault on the north, divide the island into three major tectonic blocks (Fig. 4). The southernmost part of the island is known as the Sanya Terrane and is considered to be part of the Indochina Block, whereas the northern part of Hainan Island may belong to the Cathaysian Block. The Wuzhishan Terrane, making up most of the central part of the island, was likely the southern extension of either the Yangtze Block or Cathaysian Block (Zhang et al., 1990). Abundant late Permian mafic rocks in the Wuzhishan Terrane have geochemical affinities to the Shuanggou and Babu ophiolites in South Yunnan (Yumul et al., 2007), and are likely remnants of Paleo-Tethyan oceanic crust that originally separated the South China Block from the Indochina Block (Li et al., 2006; Cai and Zhang, 2009).

2.2. Proterozoic strata

2.2.1. The southwestern Yangtze Block

Widely distributed Proterozoic strata include the Paleoproterozoic Dahongshan, Dongchuan, and Hekou Groups, the Mesoproterozoic Kunyang and Huili Groups, and the Neoproterozoic Yanbian Group in the Kangdian region (Figs. 2 and 5). Both the Dahongshan and Hekou

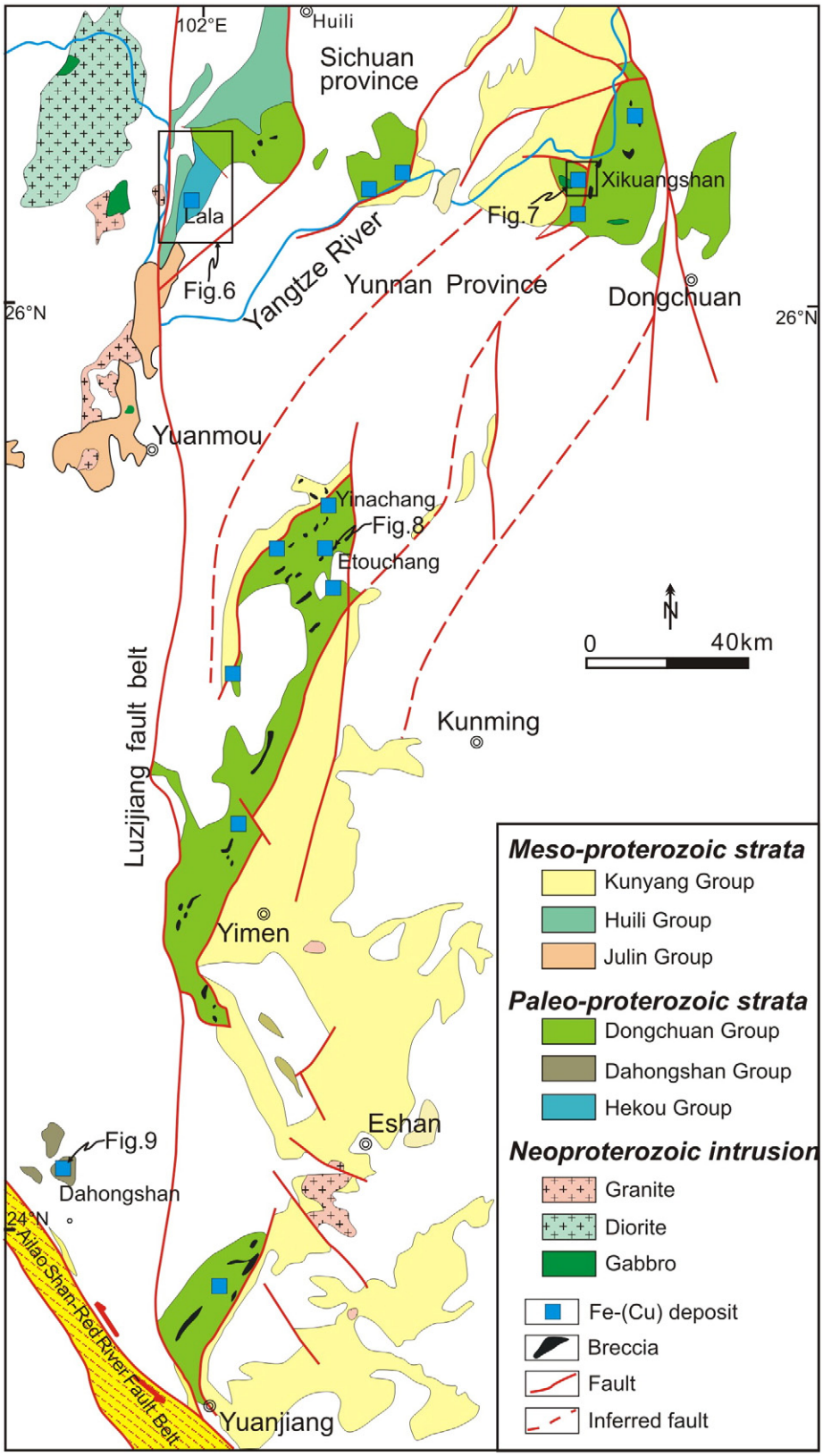

Fig. 2. Simplified geological map of the Kangdian region, SW China (modified from Wu et al., 1990; Zhao and Zhou, 2011). Major Fe–Cu deposits of the Kangdian metallogenic province are hosted in the Paleo-Mesoproterozoic strata.

Groups are composed of meta-volcanic and meta-sedimentary rocks including mica schist, carbonate, amphibolite, and meta-conglomerate (Wu et al., 1990; Hu et al., 1991; Greentree and Li, 2008). Meta-volcanic rocks of the Dahongshan Group have zircon U–Pb ages of 1.68 ± 0.01 Ga (Greentree and Li, 2008) and 1.681 ± 0.013 Ga (Zhao and Zhou, 2011). The Hekou Group contains volcanic rocks with ~1.7-Ga zircon grains (W.T. Chen et al., 2013). The Dongchuan Group, which is only weakly deformed and has undergone only low-grade

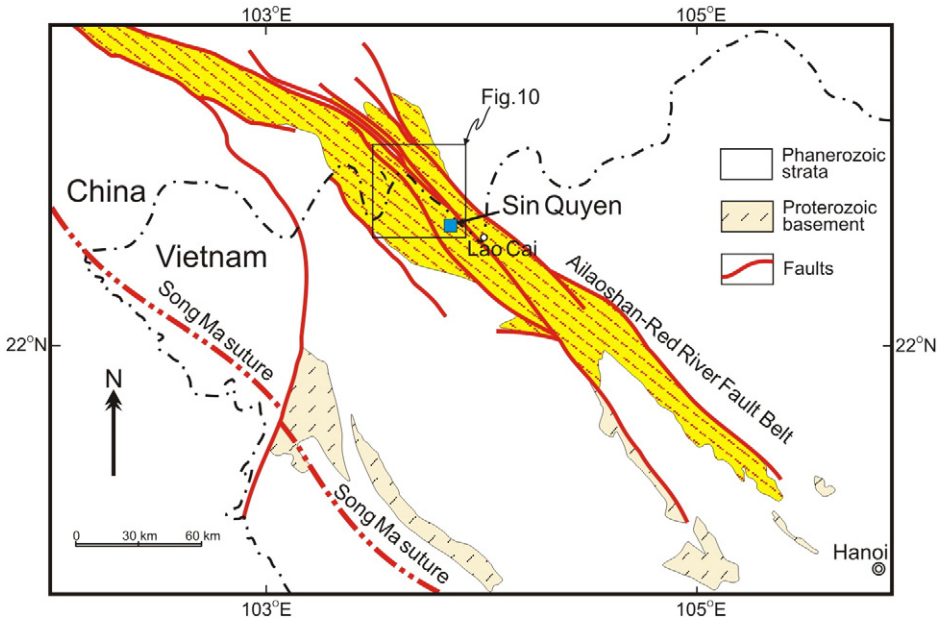

Fig. 3. Geological map of the Red River Belt, Southwest China and northern Vietnam, showing the Red River fault belt and the Song Ma suture marked by ophiolites (simplified from Hieu et al., 2012).

greenschist facies metamorphism (Wu et al., 1990), is composed of conglomerate, sandstone, and mudstone with minor volcanic rocks. Recent zircon U–Pb dating suggests that rocks of the Dongchuan Group were likely deposited at ~1.7 to 1.5 Ga (Sun et al., 2009; Zhao et al., 2010). Therefore, the Dongchuan, Dahongshan, and Hekou Groups are thought to be lateral equivalents (Fig. 5) (Zhao et al., 2010). These rocks are unconformably overlain by an 8000-m-thick, flysch-like sequence, ranging in age from Sinian to Silurian (e.g., YBGMR, 1990).

Both the Kunyang Group in Yunnan and the Huili Group in Sichuan are composed of a thick sequence of siliciclastic, volcanic, and carbonate

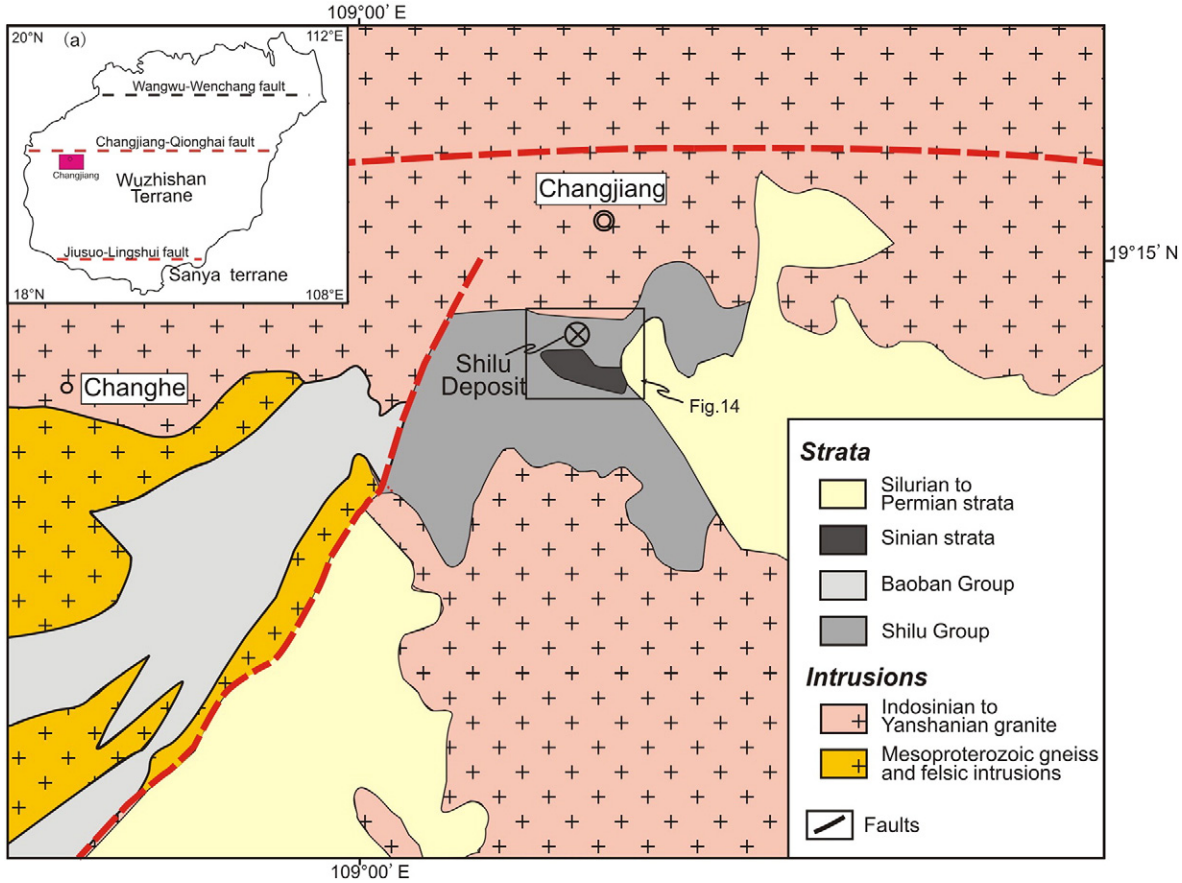

Fig. 4. Regional geological map of the Changjiang region, western Hainan Island (after Xu et al., 2007). Note that the Shilu deposit is hosted in the Shilu Group.

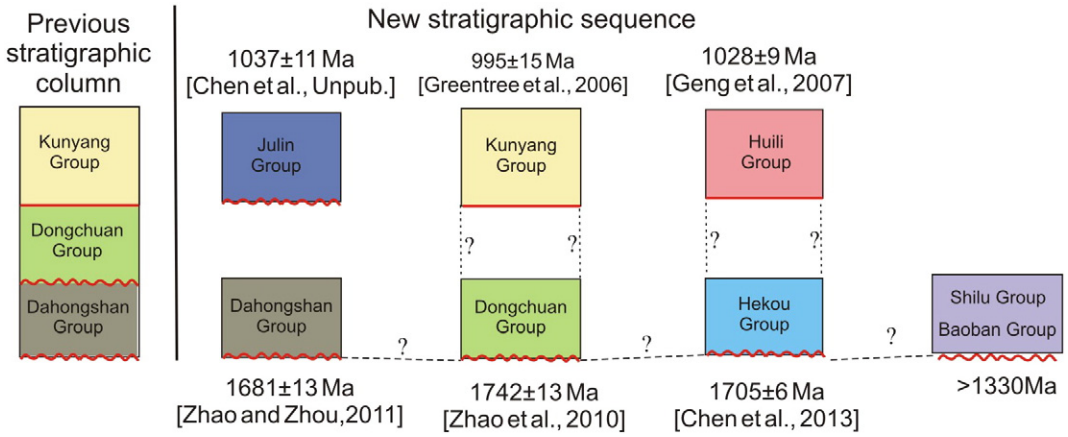

Fig. 5. Correlations of the major Proterozoic stratigraphic units of the southwestern Yangtze Block.

rocks (Wu et al., 1990), possibly deposited in a passive continental margin environment. Volcanic units in the lower parts of these groups have SHRIMP zircon U–Pb ages of ~1.0 Ga (Greentree et al., 2006; Zhang et al., 2007). The Yanbian Group is composed of a flysch-like sedimentary sequence with pillow lavas, and is intruded by 810 to 860 Ma gabbroic and granodioritic plutons (Sun et al., 2008, 2009). This unit was probably deposited in a back-arc basin at ~870 Ma and had source areas of proximal, undissected to transitional volcanic arcs of felsic to intermediate composition with ages of 900 to 920 Ma (Zhou et al., 2006; Sun et al., 2007).

2.2.2. Red River fault zone

High-grade metamorphic rocks along the Red River fault zone constitute the Ailaoshan Group in southern China and the Sin Quyen Group in northern Vietnam (Fig. 3). These rocks, which are strongly deformed and metamorphosed to the amphibolite facies, are considered to be a Proterozoic–Archean sequence that forms the basement of the Yangtze Block. In the Sin Quyen Group, two metamorphic units are recognized: a lower ~700-m-thick sequence of biotite schist, garnet–biotite gneiss, and amphibolite, and an upper ~1300-m-thick sequence of mica schist, amphibolite, quartzite, and migmatite. These units crop out as elongate, NW-trending bodies and are intruded by granitoid plutons of variable ages. The Sin Quyen Group contains zircon grains with ages of 2.7–3.0 Ga, 2.2–2.5 Ga, and 1.8 Ga (Hieu et al., 2012). These age groups are similar to those of zircons from rocks of the Dahongshan and Dongchuan Groups.

The Ailaoshan Group is similar to the Sin Quyen Group and is composed of gneiss, amphibolite, marble, and migmatite, with a thickness of more than 10 km. These rocks have undergone upper greenschist to granulite facies metamorphism (Wang and Ding, 1996). Zhai et al. (1990) reported a Sm–Nd whole-rock isochron age of 1367 ± 46 Ma for amphibolites. Both the Ailaoshan and Sin Quyen Groups are considered to be equivalent to the Dahongshan Group (Hieu et al., 2012).

2.2.3. Hainan Island

In the Wuzhishan Terrane, major Proterozoic sequences are the Baoban and Shilu Groups. Rocks of both groups crop out in western Hainan Island (Fig. 4). The Baoban Group is composed of migmatite, gneiss, and amphibolite, which are probably metamorphosed products of turbidites interbedded with mafic volcanic rocks. The protolith age of this sequence is uncertain, but it is suggested to range from 1.8 Ga to 1.45 Ga (Wang et al., 1991; Zhang et al., 1997; Xu et al., 2013).

The Shilu Group consists chiefly of greenschist-facies metamorphic rocks with a thickness of 1700–2600 m. The sequence includes schist, phyllite, slate, quartzite, and dolomite. These strata are not well dated, partly because they have been modified by younger tectonic events (Zhang et al., 1990). Diopside–tremolite schists contain zircon grains with SHRIMP ages of 1333 to 894 Ma (Xu et al., 2007, 2009, 2013). There are numerous K–Ar, and Rb–Sr ages ranging from 590 to 170 Ma. For example, Chen et al. (2006) reported Ar–Ar ages of 190 Ma for a metamorphic rock and ~130 Ma for some dykes in the region. The meaning of these ages is uncertain, but they may represent reset ages of Indosinian and Yanshanian tectonothermal events. Thus, we believe that the protolith of the Shilu Group should be older than 1.3 Ga (Fig. 5).

2.3. Proterozoic igneous activity

2.3.1. Paleoproterozoic igneous rocks

Paleoproterozoic igneous rocks in the southwestern Yangtze Block include volcanic rocks of the Dahongshan and Hekou Groups, and sparse mafic bodies intruding these strata (Greentree and Li, 2008; Zhao et al., 2010; W.T. Chen et al., 2013; Z.C. Chen et al., 2013; L. Chen et al., 2013). The volcanic rocks are mainly felsic in composition (SBGMR, 1991), and have undergone extensive albitization (Chen and Zhou, 2012). Paleoproterozoic mafic plutons are primarily composed of dolerites that have undergone upper greenschist–lower amphibolite facies metamorphism.

Sun et al. (2009) reported a SHRIMP zircon age of 1.50 ± 0.02 Ga for a tuff sample from the E'touchang Formation in the Lower Kunyang Group. Three gabbroic intrusions in the northern part of the province contain Fe–Ti–V oxide ore deposits with over 100 Mt ore reserves and are dated at ~1.5 Ga (Fan et al., 2013).

2.3.2. Mesoproterozoic igneous rocks

Mesoproterozoic igneous rocks include 1.0-Ga volcanic rocks of the Kunyang and Huili Groups and plutonic rocks intruding the Paleoproterozoic strata. Volcanic rocks in both the Kunyang and Huili Groups contain zircons with U–Pb ages of ~1.0 Ga (Greentree et al., 2006; Geng et al., 2007). Granitic intrusions with similar ages have also been identified (Li et al., 2002; Wang et al., 2012a,b).

2.3.3. Neoproterozoic igneous rocks

Neoproterozoic igneous rocks with ages ranging from ~860 to ~740 Ma are widespread in the western Yangtze Block (Zhou et al., 2002b; Li et al., 2003a), including voluminous granitic plutons, minor mafic–ultramafic intrusions, and subordinate volcanic rocks (Fig. 1). They extend for more than 700 km along a nearly north–south-trending belt (He et al., 1988; Zhou et al., 2002b). Granitic intrusions have been metamorphosed to gneissic bodies, indicating a broadly coeval, regional metamorphic event (He et al., 1988; Zhou et al., 2002b). All these plutons define the Hannan–Panxi arc (Zhou et al., 2002a).

Granitic plutons include normal arc-affinity granites and adakites with SHRIMP zircon U–Pb ages similar to those of the mafic–ultramafic

plutons (Zhou et al., 2002a,b; Zhao and Zhou, 2007). The granites have characteristics of typical I-type varieties. Adakitic plutons in the western Yangtze Block include the Xuelongbao pluton (Zhou et al., 2006) and several in the Panzhihua region (Zhao and Zhou, 2007). These plutons are considered to be typical of oceanic slab-derived adakites. In the Hannan region, the Neoproterozoic adakitic plutons are thought to have been generated by melting of newly formed, thickened, lower mafic crust (Zhao and Zhou, 2008).

In the western Yangtze Block, mafic intrusions in the Hannan–Panxi region have arc-like geochemical features, and are thought to have been derived from a mantle source modified by fluids and/or melt that originated from subducted slabs (Zhou et al., 2002a,b; Zhao and Zhou, 2007).

3. Kangdian IOCG metallogenic province

Rocks of the Paleoproterozoic Dongchuan, Hekou, and Dahongshan Groups in the Kangdian region host Fe–Cu deposits that form an important metallogenic province in China (Fig. 6) (Zhao and Zhou, 2011). In the Kangdian region, these strata crop out in an area extending for >300 km from north to south. The southern part of the metallogenic province was displaced along the Red River fault zone into northern Vietnam, where the best known example is the Sin Quyen Fe–Cu deposit (Fig. 3) (Mclean, 2002). The Shilu deposit on Hainan Island is possibly also part of the Kangdian province that was displaced further to the east during the opening of the Beipu Bay, and has mineralization styles similar to those in the Kangdian region (Xu et al., 2013).

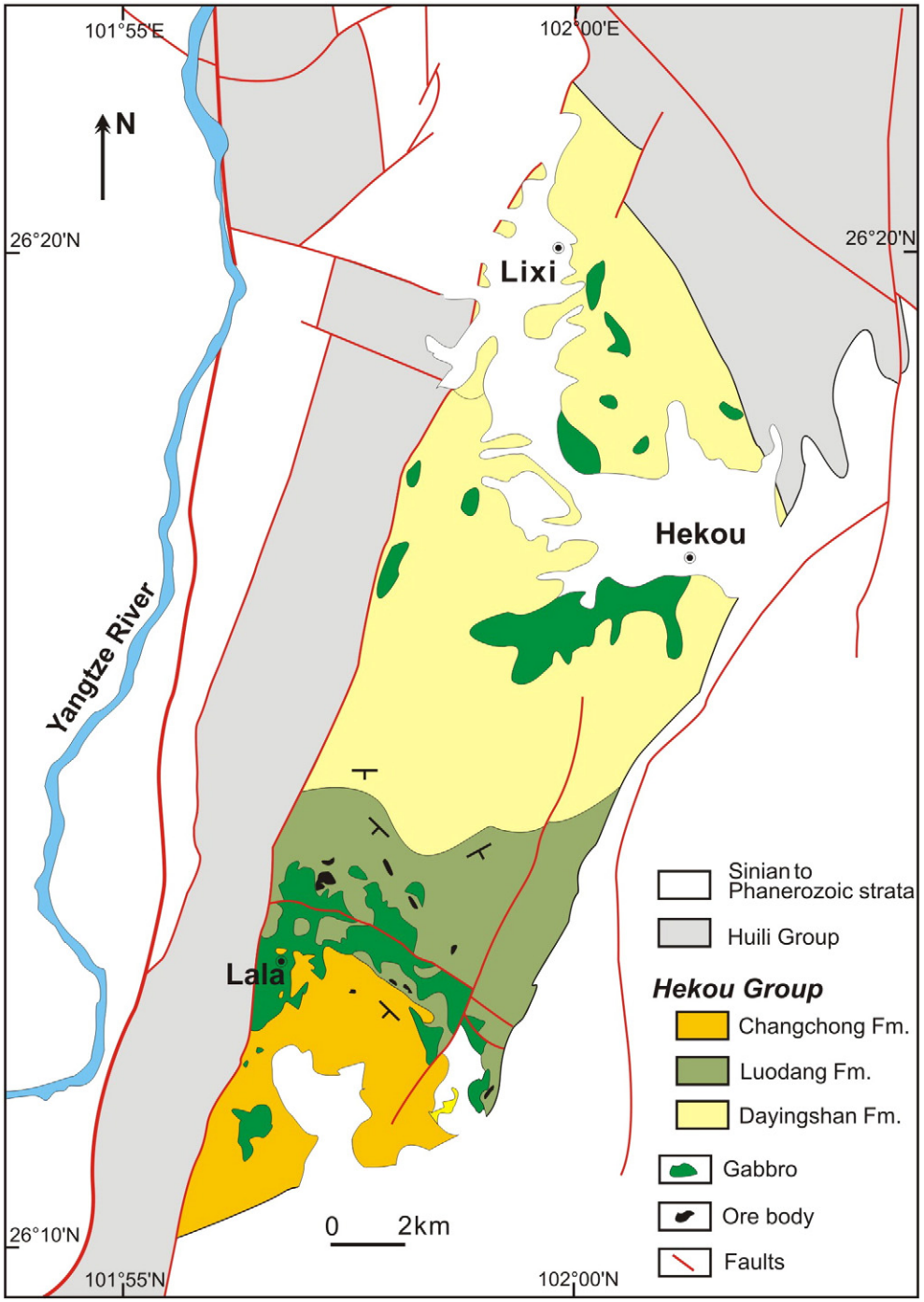

Fig. 6. Simplified geological map of the Hekou–Lala region, showing the distribution of major orebodies and mafic intrusions (after Chen and Zhou, 2012).

The Lala, Xikuangshan, Yinachang, E'touchang, and Dahongshan deposits are the largest deposits in the province (Fig. 2). Although total reserves are not available for the entire metallogenic belt, early exploration indicates a minimum of >600 Mt iron and >5 Mt copper for deposits in the Kangdian region (Qian and Shen, 1990; Sun et al., 1991a), not including the Shilu and Sin Quyen deposits, making this one of the largest IOCG provinces in the world. These Fe–Cu deposits contain Fe-oxides (magnetite and hematite) and/or Cu-sulfides (chalcopyrite and bornite) as major components, with variable amounts of Au, Ag, Co, and REE. Iron-oxides have low TiO_2 and V_2O_5, suggesting a hydrothermal origin. In these deposits, orebodies are closely associated with brecciation, as is common in IOCG deposits elsewhere (Groves et al., 2010).

3.1. Lala deposit

The Lala Fe–Cu deposit contains more than 200 million tons of ores with an average grade of 13 wt.% Fe, 0.92 wt.% Cu, 0.018 wt.% Mo, 0.022 wt.% Co, 0.25 wt.% REE_2O_3, and 0.16 ppm Au (Zhu et al., 2009). Most of the orebodies occur as irregular lenses and veins hosted in albitite, mica-schist and minor quartzite of the Hekou Group and are spatially associated with gabbroic intrusions (Fig. 6). They are roughly stratabound, striking NW–SE and dipping to the south. Some orebodies are also controlled by EW-striking lithological contacts, faults, or shear zones. Both hosting rocks and orebodies were foliated and folded along NS-trending axes and truncated by younger, steeply dipping, N–S faults. Breccias are locally present in the Lala deposit and are generally associated with orebodies.

Iron- and copper-bearing minerals occur either separately or together to form massive and disseminated oxide, sulfide, and mixed oxide–sulfide ores. Sulfide ores occur as bands and stringers or as disseminations. Stockworks and massive veins or discontinuous veinlets of sulfides are also present, crosscutting the foliated host rocks and oxide ores. In mixed oxide–sulfide ores, sulfide minerals occur either as pervasive disseminations or as banded replacements and veinlets, overprinting earlier banded and disseminated magnetite.

The paragenetic sequence in the Lala deposit includes early Na alteration followed by deposition of magnetite and magnetite-polymetallic sulfides that are overprinted by sulfide-quartz veins and finally by barren quartz-carbonate veins (Chen and Zhou, 2012). Magnetite mineralization was associated with pervasive Na–Fe alteration that formed albite, chlorite, and actinolite. Abundant Fe-, Cu-, and Mo-bearing sulfides are intergrown with angular magnetite and minor titanite, allanite, and REE minerals, and are associated with carbonate, quartz, fluorite, and mica.

3.2. Xikuangshan deposit

In the Dongchuan district, there are both of sediment-hosted stratiform copper (SSC) deposits and of Fe–Cu deposits (Fig. 7). The SSC

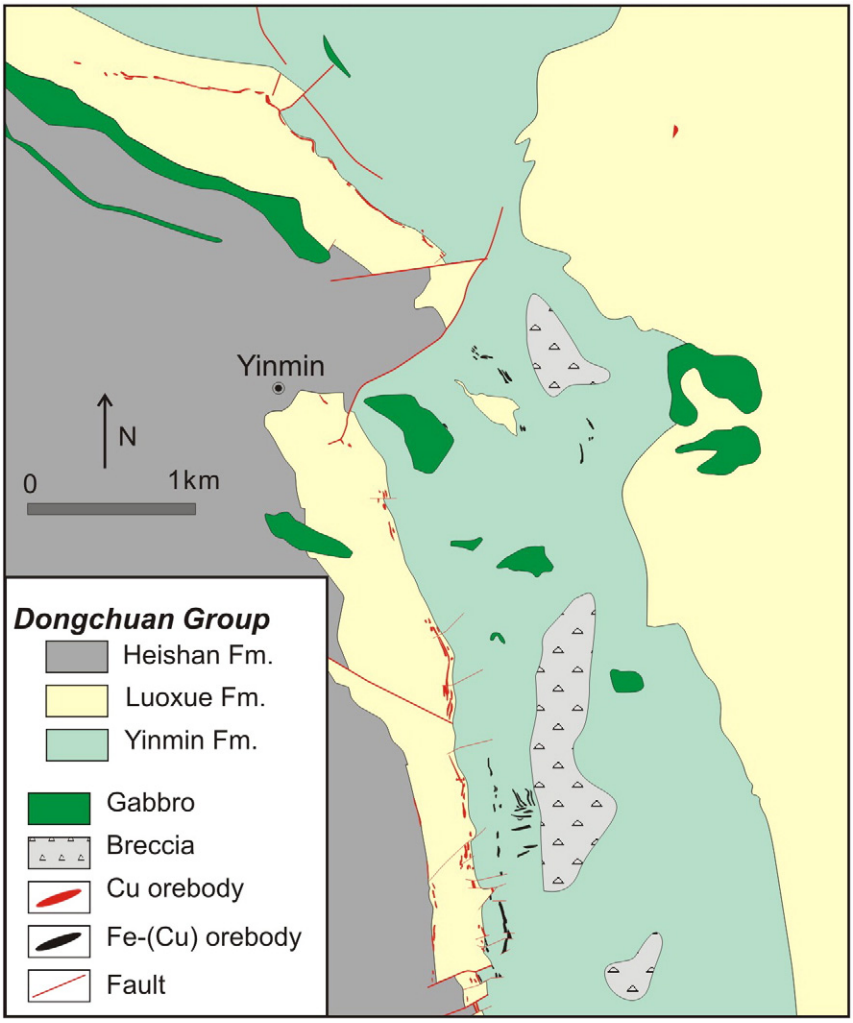

Fig. 7. Simplified geological map of the Dongchuan region, both sediment-hosted stratiform Cu and IOCG deposits are indicated (modified from Zhao et al., 2013). Note that the Fe–(Cu) orebodies are spatially associated with breccia.

deposits are hosted in carbonates of the Dongchuan Group (Zhao et al., 2012). The most famous Fe–Cu deposit is the Xikuangshan deposit that contains Fe-oxide and Cu-sulfide orebodies between the towns of Yinmin and Luoxue. The Fe–Cu orebodies are hosted in meta-siltstone/tuffaceous rocks of the Yinmin Formation, which are stratigraphically overlain by stratiform Cu orebodies. The mineralization style of both Fe–Cu and Cu orebodies was previously called "Xikuangshan-type" (Sun et al., 1991a; Gong et al., 1996). The footwall consists of sedimentary rocks of the Yinmin Formation, which are extensively overprinted by late K-feldspar, sericite, chlorite, quartz, and carbonate. Widespread breccias are closely associated with orebodies (Fig. 7). Multi-phase brecciation is evident because late breccias contain clasts of early formed breccias.

The Fe–Cu orebodies are roughly concordant with the stratification of the Yinmin Formation, but can be structurally controlled by faults or fractures and thus be locally discordant (Sun et al., 1991a). They are crosscut by a series of faults and dolerite dikes. One dolerite dyke that crosscuts a Fe–Cu orebody has zircon grains with a LA-ICP-MS U–Pb age of 1.69 Ga (Zhao and Zhou, 2011).

3.3. Yinachang and E'touchang deposits

The central part of the province hosts several deposits including the Yinachang and E'touchang deposits that are described in Zhao et al. (2013). The Yinachang deposit contains approximately 15 Mt at 0.85–0.97 wt.% Cu and 20 Mt at 41.9–44.5 wt.% Fe (unpublished exploration report, 1979, in Chinese), with anomalous amounts of Co, Mo, and REE. The E'touchang deposit is located about 20 km to the south of the Yinachang deposit. An early exploration report indicates a reserve of 16 Mt at 50 wt.% Fe, but the Cu reserve is not available due to its low grade (unpublished exploration report, 1960, in Chinese).

Both the Yinachang and E'touchang deposits are situated along regional NNE-trending faults. Orebodies are hosted in NE- or NNE-trending anticlines in rocks of the Dongchuan Group. They are commonly located in the cores of the anticlines, which were truncated by later strike-slip faults (Sun et al., 1991a,b). Orebodies are structurally controlled and occur either along fault planes or lithologic contacts. They have a close spatial association with breccia bodies of hydrothermal origin (Fig. 8).

In the E'touchang deposit, many orebodies are truncated by two, steeply dipping, NE-trending strike-slip faults. Orebodies are in sharp contact with extensively metasomatized host rocks. The hanging wall rocks are silicified and albitized. Subsidiary Cu-sulfide ores occur mostly in dolostones of the Luoxue Formation and carbonaceous rocks of the E'touchang Formation.

The E'touchang deposit contains both magnetite and hematite orebodies. Ores consist essentially of magnetite and/or hematite with local chalcopyrite, bornite, and pyrite. Siderite veins with euhedral specularite are widespread in the Fe-oxide ores. The Cu-bearing sulfides occur as veins, discontinuous veinlets, and disseminations in altered host rocks or massive magnetite bodies. Sulfides (chalcopyrite ± pyrite) commonly crosscut magnetite or early magnetite/hematite with

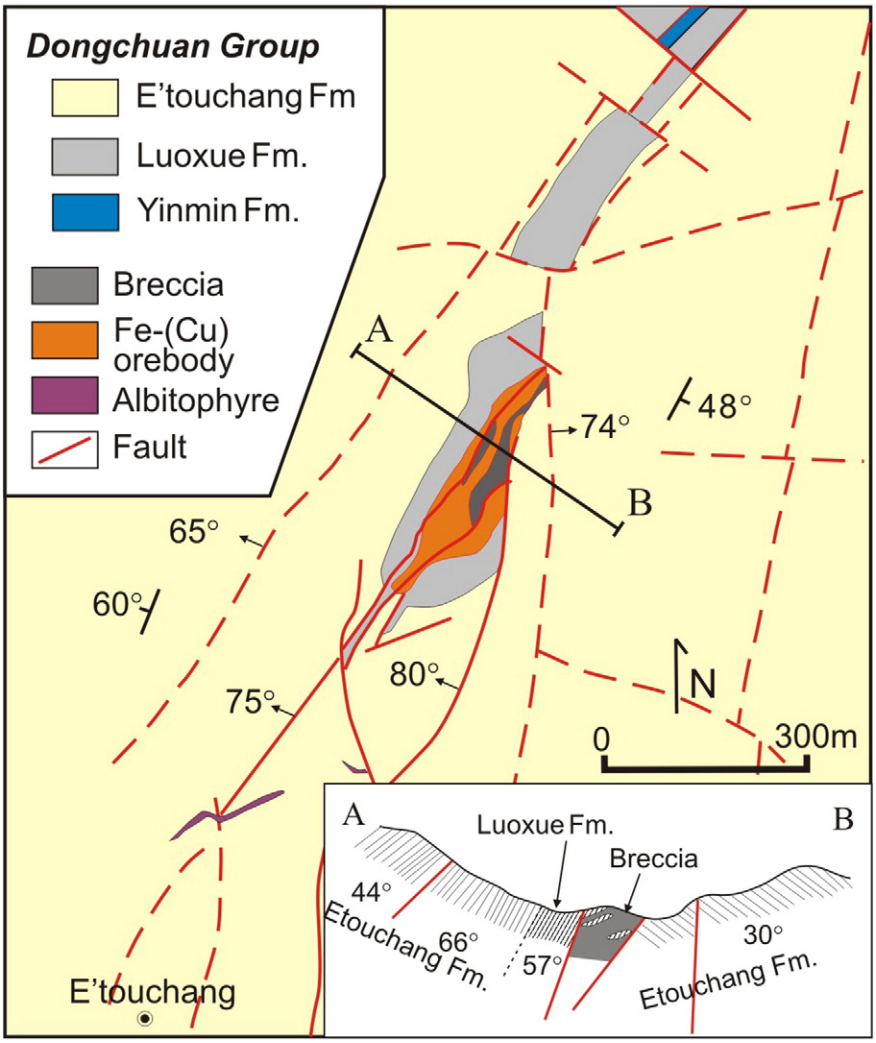

Fig. 8. Simplified geological map of the E'touchang deposit. Note that the orebodies are hosted in a breccia pipe (after Zhao and Zhou, 2011).

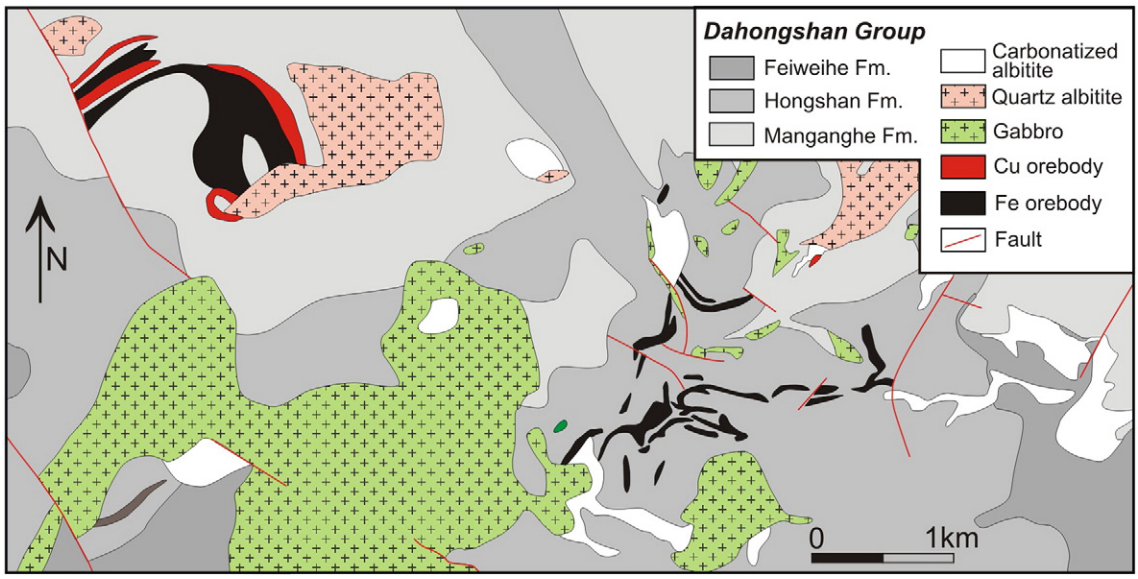

Fig. 9. Simplified geological map of the Dahongshan deposit (after Zhao and Zhou, 2011). Note that the orebodies are closely associated with gabbroic intrusions.

interstitial chalcopyrite ± pyrite. Magnetite replaced by hematite and chalcopyrite. Ductile deformation of hematite, magnetite, and chalcopyrite suggests that these minerals formed more or less simultaneously.

Albite and quartz are the most common gangue minerals in both Fe-oxide and Cu-sulfide ores. They are commonly intergrown with ore minerals, suggesting their contemporaneous formation. Pervasive sodic alteration affected almost all the rocks in the deposit, forming abundant albite. Albite alteration is overprinted by potassic (K-feldspar, sericite, biotite)-hematite alteration and minor apatite. Carbonate veins, mostly ankerite and siderite, crosscut all other rocks or ores. These veins are commonly barren, but may have minor specularite and sulfides (Zhao, 2010).

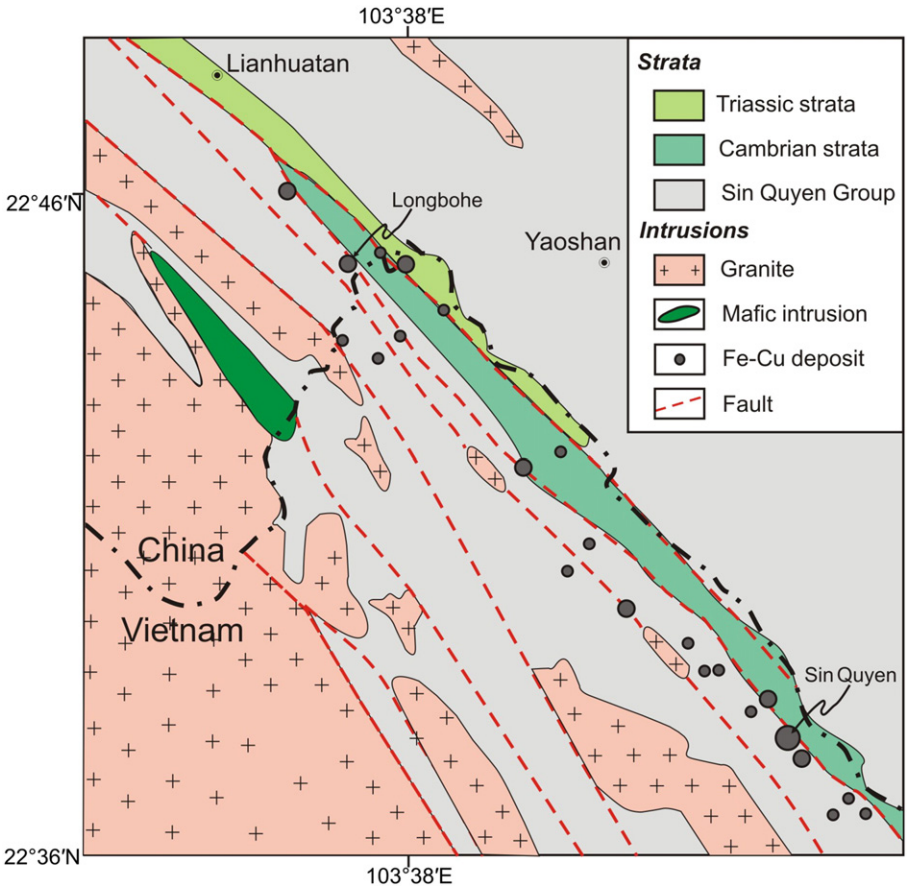

Fig. 10. Simplified geological map along the border area between northern Vietnam and southern China (after Gas'kov et al., 2012). Note that there are more than 20 Fe–Cu deposits in the Red River Belt.

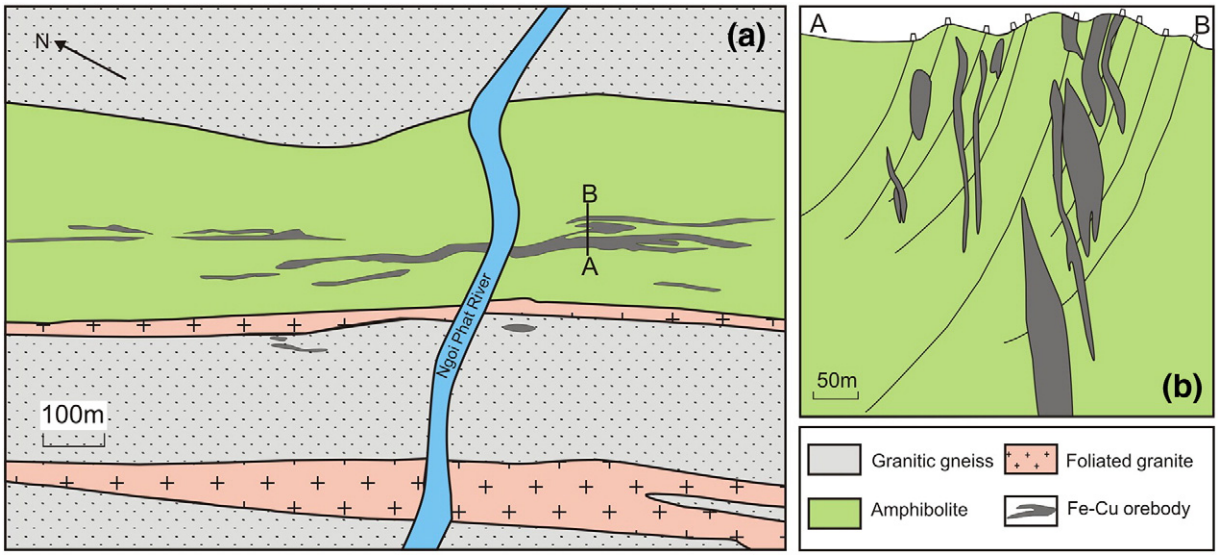

Fig. 11. (a) Simplified geologic map of the Sin Quyen deposit. Note that the orebodies hosted in amphibolite; (b) a cross-section of the Sin Quyen deposit showing the shape and distribution of orebodies (after Gas'kov et al., 2012).

3.4. Dahongshan deposit

Being the largest Fe–Cu deposit in the Kangdian region, the Dahongshan deposit has a reserve of 458.3 Mt ore at 41.0 wt.% Fe and 1.35 Mt Cu (metal), with about 15.97 t Au, 141 t Ag, 18,156 t Co, and 2.07 t Pd and Pt stated as potential by-products (unpublished exploration report of Yunnan Province, 1983). The deposit was discovered through an aeromagnetic survey in the 1960s and has been mined since the late 1990s (NGTYP, 2006). It produces nearly 30,000 t of Cu (metal) and 4 Mt of Fe (metal) annually. It is located about 10 km northeast of the Red River fault zone and about 150 km southwest of Kunming (Figs. 1 and 2).

The orebodies are hosted in rocks of the Dahongshan Group, and are closely associated with gabbroic intrusions (Fig. 9). Most of the orebodies are roughly concordant with the stratification and show crude zoning of metals. The orebodies include massive or banded magnetite ores, and stratabound disseminated or stockwork magnetite–chalcopyrite ores.

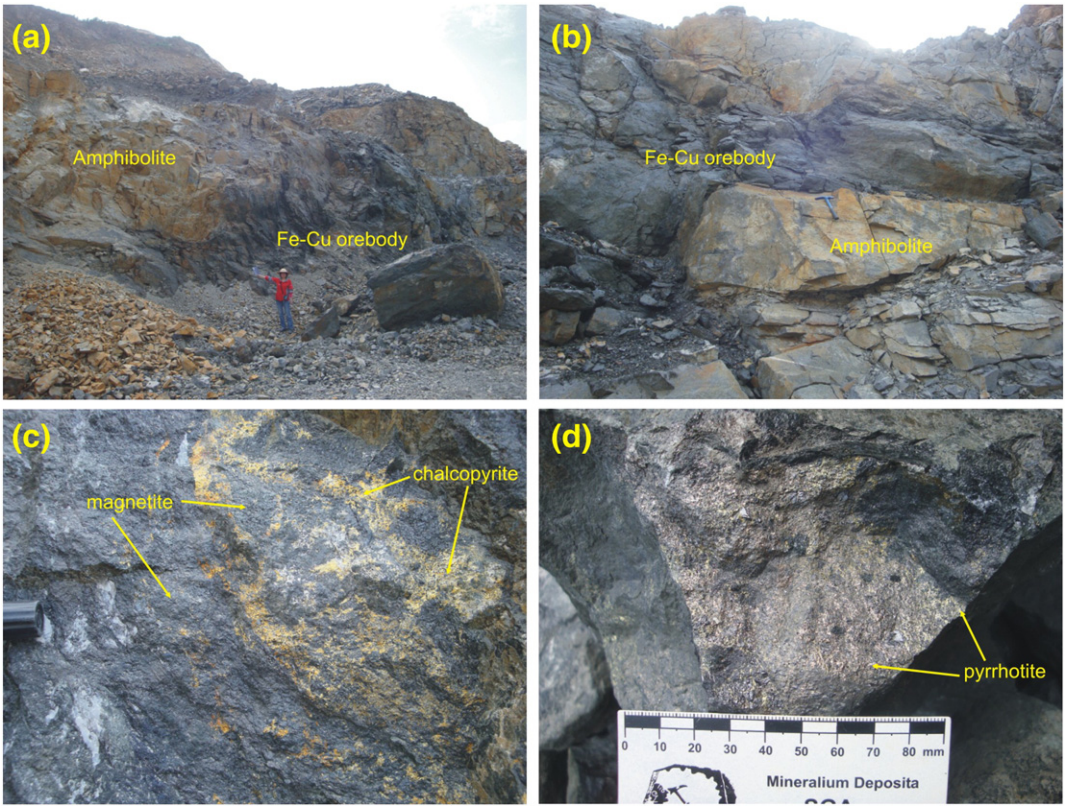

Fig. 12. Field photos of different ores in the Sin Quyen deposit, northern Vietnam. (a) and (b) Fe–Cu orebodies are hosted in amphibolite, and both orebodies and hosting rocks are extensively deformed or foliated. Note that the irregular orebodies are; (c) Fe–Cu ore. Chalcopyrite occurs as interstitial phases crosscutting earlier magnetite; (d) Fe–Cu ore. Late pyrrhotite and chalcopyrite crosscut early Fe-oxides.

Magnetite ores are hosted in metavolcanic rocks or breccia pipes, whereas magnetite–chalcopyrite ores occur predominantly as disseminations and veinlets within mica schists. These oxides are chiefly magnetite and Cu-sulfides are predominantly chalcopyrite with minor bornite. Both host rocks and ores are highly foliated.

Hydrothermal alteration associated with the Dahongshan deposit is extensive. Albite is widespread in all the country rocks and Fe-oxide ores. Locally, intermediate and felsic volcanic rocks, possibly dacite and/or andesite, of the Dahongshan Group are extensively metasomatized and recrystallized to form albitites with remnant porphyritic textures. Albitization was followed by alteration of amphibole, tourmaline, biotite, sericite, and chlorite. Pyroxenes in the dolerites have been completely replaced by amphibole. Most of the country rocks contain abundant biotite and chlorite. Late-stage patches and veins of quartz and carbonate crosscut all the lithologies, possibly indicating late-stage retrograde alteration.

3.5 . Sin Quyen deposit

The Fe–Cu deposits along the Red River fault zone include the Sin Quyen, Taphoi, Ban Vuoc, Tong Cao Chay, Suoi Thau, Nam Chac and Lung Po deposits in northern Vietnam; the Longbohe deposit of Yunnan Province, China, is also within the fault zone (Fig. 10) (Gu et al., 2007; Cui, 2008). The Sin Quyen deposit has anomalous amounts of Au and REE and is hosted in the Sin Quyen Group.

Major orebodies of the Sin Quyen deposit are distributed over an area 140-m-wide and ~2-km-long (Fig. 11). There are seventeen lenticular and sheet-like orebodies, either concordant or subconcordant with the host rocks (Fig. 12a–b). These orebodies vary in thickness from a few tens of centimeters to 25 m and are as much as 4000-m-long. Orebodies are commonly brecciated, fragmented, and boudinaged, and occur chiefly as irregular lenses and veins due to the shearing of the Red River fault zone (Fig. 11). The total ore reserves are ~50 million

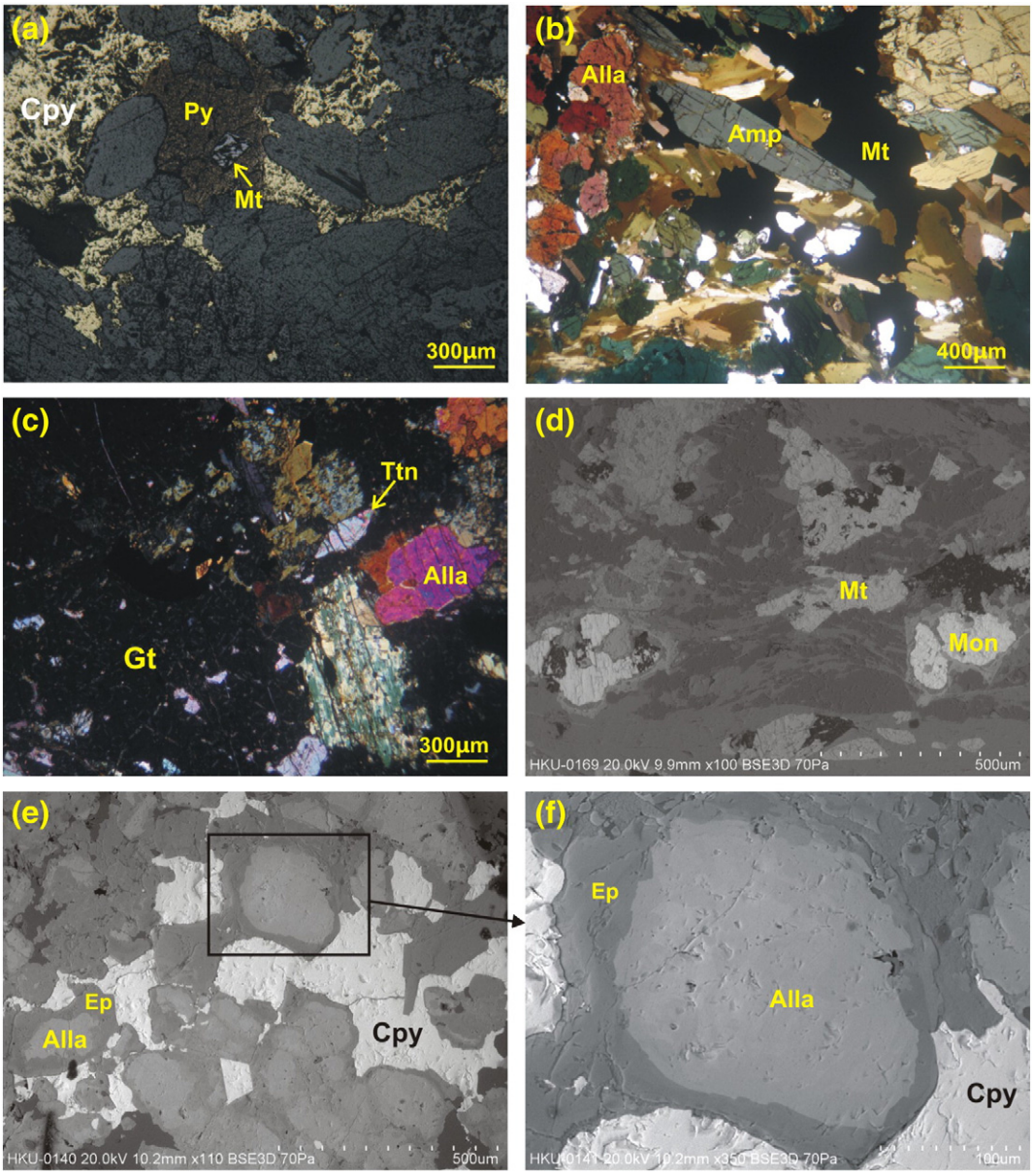

Fig. 13. Micro-photos of different ores in the Sin Quyen deposit. (a) Oxide ore is mainly composed of subhedral to euhedral magnetite, amphibole and allanite with minor interstitial chalcopyrite and pyrite; (b) large amounts of REE-bearing allanite coexisting with magnetite and amphibole; (c) garnet is associated with titanite and allanite; (d) monazite is associated with magnetite; (e) chalcopyrite occurs as interstitially along with allanite; (f) rectangle zone in Fig. (e), showing that REE-poor epidote grows around the REE-rich allanite. Abbreviations: Cpy — chalcopyrite; Py — pyrite; Mt — magnetite; Alla — allanite; Amp — amphibole; Gt — garnet; Ttn — titanite; Mon — monazite; Ep — epidote.

tons with average ore grades of ~1 wt.% Cu, 14 wt.% Fe, and 0.5 g/t Au (Gas'kov et al., 2012).

The ores have highly variable abundances of minerals and include sulfide and sulfide–oxide ores (Fig. 12c–d). Sulfide ores consist of pyrite, pyrrhotite, and chalcopyrite (Fig. 12d), whereas sulfide–oxide ores are composed of chalcopyrite and magnetite (Fig. 12c). They are mainly disseminated, banded, or massive, and locally are highly deformed or foliated. Chalcopyrite and pyrite often occur interstitially along margins of magnetite, indicating that the sulfides were generally later than the oxides (Figs. 12c and 13a).

In addition to chalcopyrite, magnetite, pyrite, and pyrrhotite, minor gold and REE minerals are also present (Fig. 13b–f). Some sulfide ores contain Au and Ag up to 2 g/t, with native gold occurring as fine (<0.1 mm), bright yellow segregations, mainly tabular and hackly and sometimes lumpy (Gas'kov et al., 2012). The common REE minerals are allanite and orthite $(Ca,Ce,La,Y)_2[SiO_4](OH)$, with minor bastnaesite $(Ce, La)[CO_3]F$, titanite, and monazite $(Ce,La)[PO_4]$ (Fig. 13b–f).

Gas'kov et al. (2012) propose that the formation of the Sin Quyen deposit occurred synchronously with deposition of the hosting strata because the Fe–Cu mineralization is concordant with the host rocks. Because the protolith of host amphibolites was interpreted to be volcanic in origin, the association of Fe–Cu mineralization with volcanic rocks led Gas'kov et al. (2012) to propose that the mineralization is a Cyprus type massive sulfide deposit.

3.6. Shilu deposit

The Shilu deposit on Hainan Island has a giant reserve of more than 460 Mt of hematite-rich ores at an average grade of 51% FeO, associated with economic Cu, Co, Ni, Ag, Pb and Zn (Xu et al., 2013). Orebodies are hosted in low-grade metamorphosed, although locally up to amphibolite facies, volcaniclastic sedimentary rocks and carbonates, and high-grade, diopside-tremolite-bearing, gneissic rocks of the Shilu Group (Fig. 14). The orebodies are all structurally controlled (Xu et al., 2013).

There are iron-oxide ores, Cu–Co-sulfide ores, and mixed oxide–sulfide ores in the Shilu deposit (Fig. 14). Iron-oxide ores are massive, semi-massive or disseminated. Massive ores are composed of hematite (~85%), magnetite (~1%), quartz (~14%), barite (1%), and sericite (1%) (Fig. 15a–b). Other semi-massive or disseminated iron ores are composed of hematite (20%–40%), magnetite (20%–45%), garnet (20%–25%), quartz (0%–19%), feldspar (0%–5%), diopside, and tremolite (0%–4%), with minor epidote, chlorite, calcite, dolomite, allanite, titanite, barite, biotite, and sphene (Figs. 15c–d and 16a–c). The Cu–Co-sulfide ores are hosted mainly within dolostones and banded dolostones, about 30–60 m below the iron-oxide orebodies. They are massive or disseminated, containing Co-bearing pyrite, Co-bearing pyrrhotite, and chalcopyrite (Fig. 16d). In mixed oxide–sulfide ores, Cu–Co-rich sulfides occur as interstitial phases or crosscut earlier iron-oxides (Fig. 15e–f). In both Fe-oxide and Cu–Co-sulfide ores, quartz grains are recrystallized to sub-grains (Fig. 16a), whereas magnetite and sulfides are slightly to moderately elongated (Fig. 15). Alteration and metamorphism resulted in extensive development of skarns, containing diopside, epidote, tremolite, actinolite, K-feldspar, epidote, chlorite, silica, and carbonate.

4. $^{40}Ar/^{39}Ar$ dating results

Biotite and amphibole separates from Fe–Cu ores and ore-hosting strata of the Dahongshan, Yinachang, Xikuangshan, and Lala deposits were used for $^{40}Ar/^{39}Ar$ dating. Samples were crushed in a stainless

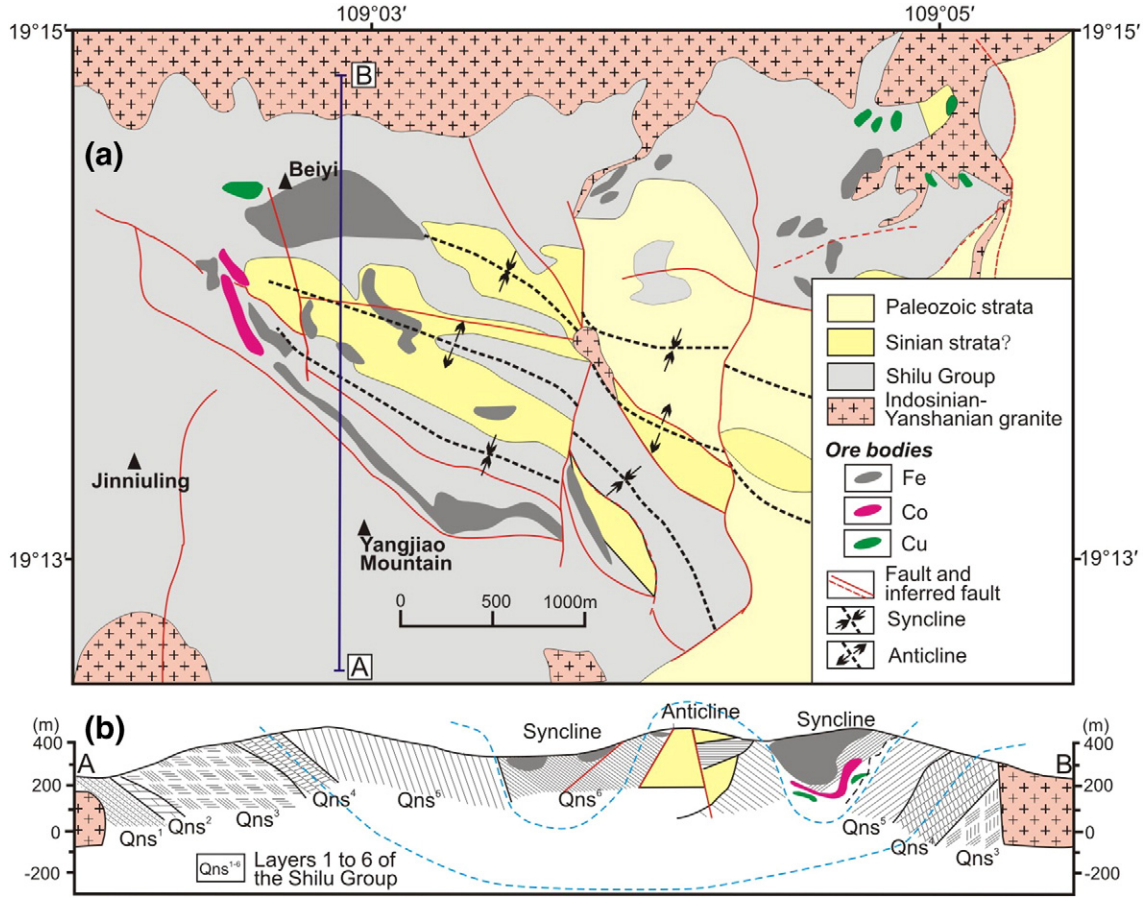

Fig. 14. (a) Simplified geological map of the Shilu deposit showing the distributions of different orebodies (modified from Xu et al., 2013); (b) a cross-section showing the occurrence of orebodies in the hosting Shilu deposit.

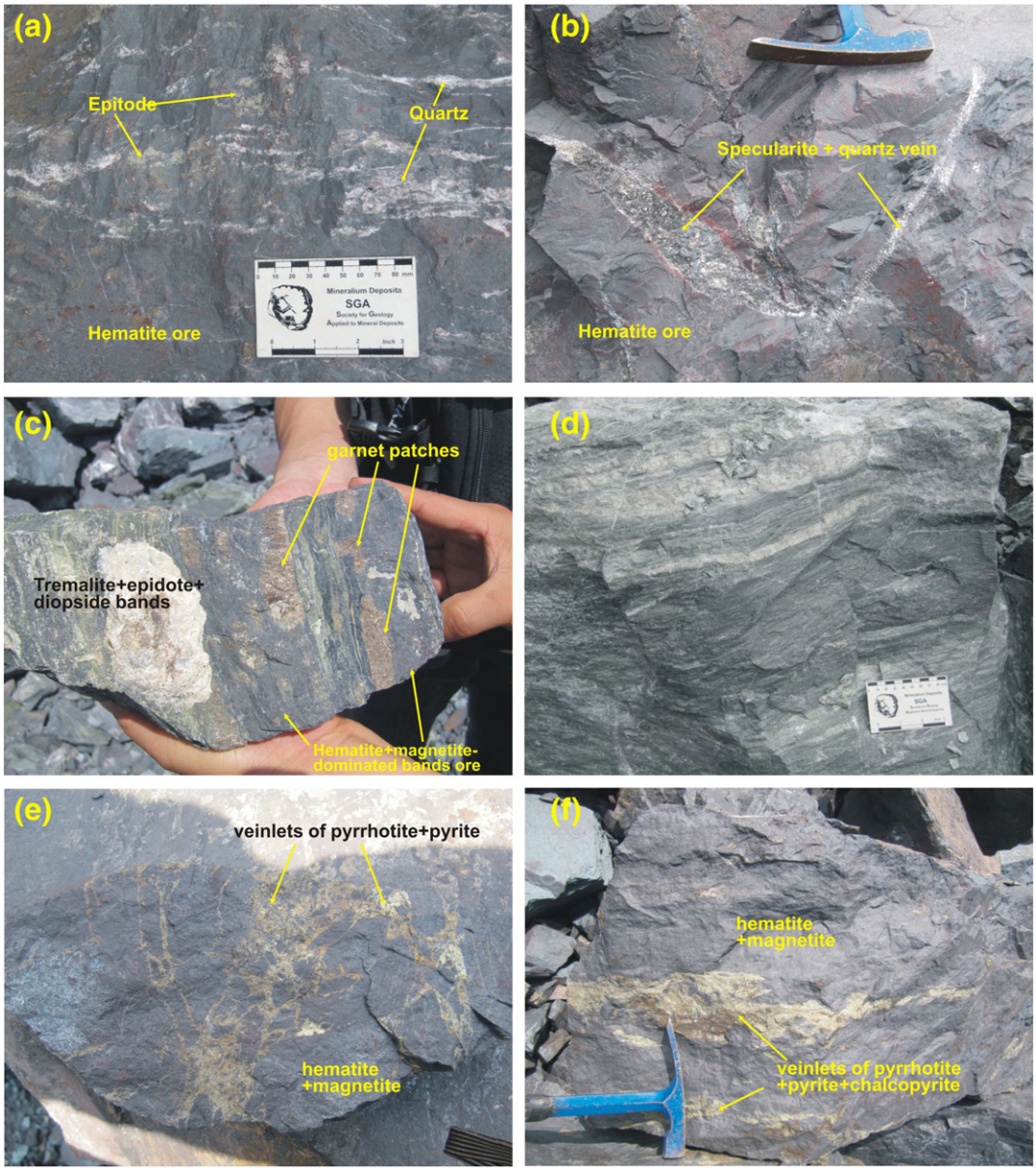

Fig. 15. Field photos of different ores in the Shilu deposit. (a) Massive hematite ores crosscut by veinlets of quartz and epidote; (b) massive hematite ores crosscut by veins of specularite and quartz; (c) banded ores containing bands of tremolite, epidote, diopside, iron oxides and garnet; (d) banded hosting rocks composed of dominantly chlorite and tremolite; (e) and (f) early Fe-oxide ores crosscut by late veinlets of pyrrhotite and pyrite. Note that the ores are generally deformed.

steel mortar and then cleaned in an ultrasonic bath with deionized water for 15 min. Pure biotite and amphibole separates were hand-picked under a binocular microscope. Biotite separates were irradiated along with the ZBH-25 biotite standard (132.7 ± 0.1 Ma) for 54 h at the 49-2 reactor, Chinese Academy of Science. After a 3-month cooling period, the samples were analyzed by the $^{40}Ar/^{39}Ar$ laser heating method using a GV5400 mass spectrometer equipped with a MIR10-50W CO_2 laser. Analytical procedures are available in Qiu and Jiang (2007). Argon gas was extracted at consecutively higher laser powers at each designated power. Released gases were purified by two Zr–Al getter pumps operated for 5 to 8 min at room temperature and ca. 450 °C. The $^{40}Ar/^{39}Ar$ results are calculated and plotted using the ArArCALC software of Koppers (2002). All dates are reported using 5.543×10^{-10} a^{-1} as the total decay constant for ^{40}K (Steiger and Jäger, 1977), and correction factors for interfering argon isotopes derived from Ca and K are: $(^{39}Ar/^{37}Ar)_{Ca} = 8.984 \times 10^{-4}$, $(^{36}Ar/^{37}Ar)_{Ca} = 2.673 \times 10^{-4}$ and $(^{40}Ar/^{39}Ar)_{K} = 5.97 \times 10^{-3}$. The age errors are reported at the 95% confidence level (2σ), and include the errors in the irradiation correction factors, but do not include the uncertainty of the potassium decay constant.

New $^{40}Ar/^{39}Ar$ analytical data are summarized in Table 1 and the apparent age spectra are illustrated in Fig. 17. All the samples have similar age spectra characterized by anomalously young ages at initial steps, which progressively increase to a plateau at steps of high temperatures (Fig. 17). Plateau ages are calculated using the weighted mean average of 5–10 contiguous heating steps that account for more than 50% of the total ^{39}Ar released; except for sample YN07-297, which has a pseudo plateau with 4 contiguous steps accounting for 30–35% of the total ^{39}Ar.

One amphibole sample from amphibolite (YN07-192) and one biotite sample from garnet-biotite schist (YN07-223) were collected from the Dahongshan deposit. The amphibole and biotite separates have plateau ages of 831 ± 20 Ma and 851 ± 9 Ma, respectively (Fig. 17). The two ages are identical within uncertainties and can be considered as the metamorphic age of the Dahongshan Group.

Biotite separates were also collected from a chalcopyrite–carbonate–quartz vein (YN07-297) of the Yinachang deposit. It has a pseudo

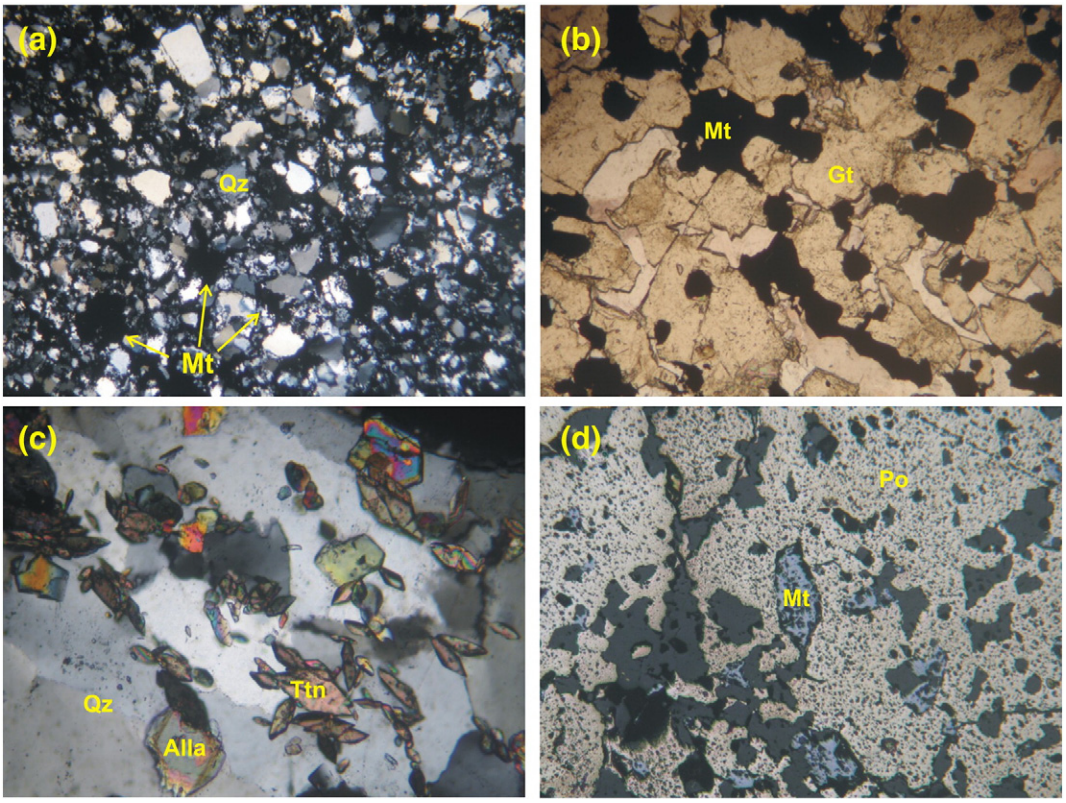

Fig. 16. Micro-photos of different ores from the Shilu deposit. (a) Oxide ores are composed of mainly subhedral magnetite and quartz; (b) magnetite appears interstitially within garnet; (c) minor titanite and allanite occur together with quartz; (d) in sulfide ore, early magnetite is enclosed by late pyrrhotite. Abbreviations: Qz — quartz; Mt — magnetite; Gt — garnet; Ttn — titanite; Alla — allanite; Po — pyrrhotite.

plateau age of 831 ± 9 Ma (Fig. 17), and is considered to be the best estimate for the cooling age of the biotite sample. Biotite from a quartz–carbonate vein (DC-26) that crosscuts the ore-hosting strata in the Xikuangshan deposit has a plateau age of 820 ± 8 Ma. The age constitutes more than 80% radiogenic Ar, which can best represent the cooling age of the sample. This age is identical to that of biotite from the Yinachang deposit.

Biotite separates from samples LLZ-26 and LLZ-27 from chalcopyrite–quartz–carbonate veins of the Lala deposit have identical plateau ages of 817 ± 7 Ma and 825 ± 7 Ma (Fig. 17). The two ages account for more than 85% radiogenic Ar, and thus represent the cooling time of the sample. Both ages are also in good agreement with the ^{40}Ar–^{39}Ar ages of biotite from quartz–carbonate veins from the Yinachang and Xikuangshan deposits.

5. Multiple tectonothermal events in the Kangdian IOCG province

It was generally believed that the Fe–Cu deposits in the Kangdian province had similar origins and formed in the same environment based on their similar mineralization styles. They were considered to be either volcanic-hosted massive sulfide deposits (VHMS) or sedimentary exhalative deposits (SEDEX) in the Chinese literature (Sun et al., 1991a,b). However, their field relationships and mineralization styles are similar to many IOCG deposits (Zhao and Zhou, 2011; Chen and Zhou, 2012; Zhao et al., 2013).

Previous Pb–Pb and Rb–Sr ages of these deposits, obtained before the 1990s, range from Paleoproterozoic to Neoproterozoic (Sun et al., 1991a; Chen and Ran, 1992). The reliability of these ages is uncertain and difficult to evaluate. However, recently obtained Re–Os age dates and zircon U–Pb ages for the Yinachang, Dahongshan, and Lala deposits in the Kangdian province suggest three distinct mineralization events at 1.65 Ga, 1.45 Ga, and 1.0 Ga (Zhao and Zhou, 2011; Chen and Zhou, 2012; Zhao et al., 2013). There was a widespread Neoproterozoic tectonothermal event that affected the whole western Yangtze Block, likely related to subduction along the margin of the block (Zhou et al., 2002b). This post-ore event is well constrained by previous dates and our new $^{40}Ar/^{39}Ar$ dates of biotite and amphibole from the Fe–Cu deposits (Figs. 17 and 19).

5.1. Multiple mineralization events

Zhao et al. (2013) obtained molybdenite Re–Os model ages of ~1.66 Ga for Fe–Cu ores, and molybdenite Re–Os ages of ~1.45 Ga for hydrothermal veins from the Yinachang deposit. They interpret the older age as representing a major ore-forming event in a continental rift of the Kangdian region, whereas the younger age is thought to represent a subordinate hydrothermal event. The ~1.66 Ga molybdenite of the Yinachang deposit is synchronous with the Dahongshan deposit that was constrained by using zircon U–Pb ages of hosting volcanic rocks and dolerites intruding Fe–Cu orebodies (1.66 Ga; Zhao and Zhou, 2011). The ~1.66 Ga event was contemporaneous with, or slightly younger than, deposition of the host rocks of the Dongchuan and Dahongshan Groups. The good agreement between zircon U–Pb and molybdenite Re–Os ages suggests a regional IOCG mineralization event at ~1.66 Ga (Fig. 19).

The ~1.45 Ga hydrothermal event was not previously known in the Kangdian IOCG province, but roughly coincides with the crystallization of the ~1.50 Ga volcanic rocks of the Heishan Formation and mafic intrusions (Sun et al., 2009; Geng et al., 2012; Fan et al., 2013). The 1.45 Ga hydrothermal activity may have been associated with this magmatic event that caused local hydrothermal activity. Due to the large time gap between the ~1.66 Ga and ~1.45 Ga events (~200 Myr), it is likely that the ~1.45 Ga event represents separate hydrothermal overprint rather than a continuous process.

The Lala deposit in the northern part of the metallogenic province has molybdenite Re–Os ages of ~1.05 Ga (Li et al., 2003b; Chen

Table 1
$^{40}Ar/^{39}Ar$ dating results of biotite and amphibole of IOCG deposits from the Kangdian region.

Run ID	Laser	$^{36}Ar_{air}$	$^{37}Ar_{ca}$	$^{38}Ar_{cl}$	$^{39}Ar_{k}$	$^{40}Ar^{*}$	Age	±2 s	$^{40}Ar^{*}$	$^{39}Ar_{k}$	K/Ca
							(Ma)		(%)	(%)	
Dahongshan deposit											
YN07-192 (J = 0.0053573 ± 0.0000268)											
09G2258B	4.1%	0.000141	0.000301	0.000001	0.000053	0.005464	798.1	±214.8	11.6	2.7	0.098
09G2258C	4.3%	0.000057	0.000729	0.000001	0.000063	0.004728	612.0	±63.1	21.9	3.2	0.048
09G2258D	4.6%	0.000047	0.000932	0.000004	0.000148	0.011243	616.0	±28.5	44.8	7.5	0.089
09G2258E	5.0%	0.000045	0.007876	0.000036	0.000479	0.051026	814.3	±14.9	79.2	24.1	0.034
09G2258F	5.4%	0.000031	0.008513	0.000032	0.000452	0.049449	832.4	±15.1	84.5	22.8	0.030
09G2258H	5.8%	0.000015	0.003479	0.000013	0.000232	0.025266	828.7	±29.4	85.4	11.7	0.037
09G2258I	6.2%	0.000010	0.001955	0.000008	0.000205	0.023312	857.1	±39.6	88.5	10.3	0.059
09G2258J	6.6%	0.000010	0.003410	0.000013	0.000215	0.025342	881.5	±31.0	89.3	10.9	0.035
09G2258K	7.0%	0.000008	0.001179	0.000005	0.000073	0.006081	665.4	±69.3	71.0	3.7	0.035
09G2258L	8.0%	0.000006	0.000382	0.000001	0.000035	0.001780	432.6	±97.7	49.0	1.8	0.052
09G2258M	12.0%	0.000004	0.000256	0.000001	0.000029	0.001270	379.8	±110.6	49.5	1.5	0.063
YN07-223 (J = 0.0054750 ± 0.0000274)											
09G2259B	4.0%	0.000218	0.000000	0.000020	0.000439	0.037138	687.0	±40.2	36.5	4.0	
09G2259C	4.1%	0.000035	0.000002	0.000017	0.000274	0.027266	783.5	±12.0	72.2	2.5	78.0
09G2259D	4.2%	0.000068	0.000000	0.000056	0.000961	0.100390	816.2	±6.7	83.3	8.8	78.0
09G2259E	4.4%	0.000047	0.000001	0.000071	0.001154	0.123172	830.1	±4.7	89.9	10.5	741.6
09G2259F	4.6%	0.000013	0.000000	0.000037	0.000607	0.068249	865.0	±7.4	94.6	5.5	741.6
09G2259G	4.7%	0.000019	0.000000	0.000056	0.000889	0.099393	861.5	±5.8	94.6	8.1	741.6
09G2259I	4.9%	0.000016	0.000000	0.000053	0.000854	0.094874	857.1	±4.9	95.2	7.8	741.6
09G2259J	5.1%	0.000014	0.000001	0.000067	0.001072	0.118483	853.8	±5.2	96.6	9.8	893.0
09G2259K	5.4%	0.000014	0.000000	0.000065	0.001037	0.115087	856.7	±4.8	96.6	9.5	893.0
09G2259L	5.7%	0.000010	0.000001	0.000049	0.000790	0.086546	847.5	±7.4	96.8	7.2	541.5
09G2259M	6.1%	0.000016	0.000002	0.000084	0.001352	0.147627	845.6	±4.2	96.9	12.3	381.8
09G2259N	6.5%	0.000007	0.000002	0.000021	0.000342	0.036813	835.4	±9.1	95.0	3.1	112.6
09G2259O	7.0%	0.000008	0.000000	0.000014	0.000232	0.024963	837.0	±16.2	91.8	2.1	112.6
09G2259P	9.0%	0.000011	0.000000	0.000043	0.000696	0.074955	836.3	±6.7	96.0	6.3	112.6
09G2259Q	2.0%	0.000008	0.000000	0.000017	0.000270	0.028896	831.5	±13.7	92.4	2.5	112.6
Yinachang deposit											
YN07-297 (J = 0.0056494 ± 0.0000282)											
09G2261B	4.0%	0.000097	0.000000	0.000004	0.000096	0.007604	669.0	±53.3	20.9	0.3	156.7
09G2261C	4.1%	0.000074	0.000001	0.000004	0.000108	0.008715	679.4	±32.9	28.5	0.3	88.3
09G2261D	4.3%	0.000056	0.000003	0.000016	0.000714	0.058386	684.8	±7.4	78.0	2.0	121.0
09G2261E	4.4%	0.000024	0.000003	0.000020	0.000955	0.077415	680.3	±5.2	91.6	2.6	204.3
09G2261F	4.6%	0.000021	0.000004	0.000039	0.001934	0.163441	704.2	±3.4	96.4	5.3	242.0
09G2261H	4.8%	0.000040	0.000003	0.000101	0.004672	0.411394	728.4	±2.9	97.2	12.8	785.2
09G2261I	5.0%	0.000028	0.000002	0.000110	0.004508	0.410657	748.9	±2.9	98.0	12.3	1088.9
09G2261J	5.2%	0.000014	0.000001	0.000123	0.004343	0.410361	771.7	±2.9	98.9	11.9	1974.0
09G2261K	5.4%	0.000014	0.000000	0.000132	0.003987	0.390027	793.7	±3.1	98.9	10.9	1974.0
09G2261L	5.6%	0.000018	0.000001	0.000166	0.003898	0.408207	838.4	±3.2	98.7	10.7	2172.1
09G2261N	6.2%	0.000004	0.000001	0.000112	0.002751	0.283644	828.0	±3.7	99.5	7.5	2420.6
09G2261O	6.8%	0.000006	0.000000	0.000119	0.002916	0.300138	827.0	±3.5	99.3	8.0	2420.6
09G2261P	7.5%	0.000007	0.000001	0.000129	0.003105	0.321425	830.8	±3.2	99.3	8.5	2449.3
09G2261Q	9.0%	0.000004	0.000000	0.000020	0.000851	0.076476	740.9	±5.8	98.6	2.3	2449.3
09G2261R	12.0%	0.000002	0.000001	0.000037	0.001675	0.148103	731.0	±4.2	99.6	4.6	728.8
Xikuangshan deposit											
DC-26 (J = 0.0070000 ± 0.0000350)											
09G2267C	4.2%	0.000851	0.000012	0.000010	0.000783	0.060885	783.9	±49.1	19.4	0.6	35.6
09G2267D	4.4%	0.004561	0.000269	0.000037	0.004180	0.305961	746.4	±44.2	18.5	3.1	8.7
09G2267E	4.5%	0.002384	0.000485	0.000046	0.004847	0.369484	771.5	±20.0	34.4	3.6	5.6
09G2267F	4.6%	0.001727	0.000462	0.000054	0.005837	0.463780	797.8	±12.0	47.6	4.3	7.0
09G2267H	4.8%	0.001812	0.000638	0.000070	0.007527	0.601099	801.1	±10.2	52.8	5.6	6.6
09G2267I	5.0%	0.001989	0.001291	0.000083	0.009475	0.760409	804.3	±8.7	56.4	7.0	4.1
09G2267J	5.2%	0.002075	0.001621	0.000091	0.010366	0.842050	812.2	±8.3	57.8	7.6	3.5
09G2267K	5.4%	0.002057	0.002138	0.000109	0.011876	0.975057	819.2	±7.4	61.6	8.7	3.1
09G2267L	5.7%	0.001614	0.002030	0.000080	0.008575	0.702057	817.3	±8.1	59.5	6.3	2.4
09G2267M	6.0%	0.002110	0.002041	0.000092	0.010213	0.841819	821.8	±8.6	57.4	7.5	2.8
09G2267N	6.5%	0.002570	0.002098	0.000116	0.012764	1.055740	824.1	±8.3	58.1	9.4	3.4
09G2267O	7.0%	0.002712	0.001017	0.000133	0.014718	1.220034	825.5	±7.7	60.3	10.8	8.1
09G2267P	8.0%	0.003122	0.000223	0.000194	0.020518	1.709437	828.9	±6.5	64.9	15.1	51.5
09G2267Q	9.0%	0.001439	0.000194	0.000131	0.014036	1.171844	830.3	±5.0	73.3	10.3	40.5
Lala deposit											
LLZ-26 (J = 0.0070000 ± 0.0000350)											
09G2265C	4.2%	0.000209	0.000009	0.000004	0.000241	0.015448	667.7	±48.4	20.0	0.2	14.9
09G2265D	4.4%	0.000110	0.000012	0.000034	0.002041	0.162664	799.8	±4.9	83.3	1.9	96.2
09G2265E	4.6%	0.000165	0.000021	0.000047	0.002755	0.220854	803.6	±4.7	81.9	2.6	72.9
09G2265F	4.8%	0.000227	0.000063	0.000104	0.005714	0.460213	806.7	±3.5	87.2	5.3	50.6
09G2265H	5.2%	0.000112	0.000088	0.000098	0.005174	0.420181	812.0	±3.2	92.6	4.8	32.8
09G2265I	5.4%	0.000105	0.000197	0.000259	0.013856	1.131116	815.4	±2.8	97.3	12.8	39.4
09G2265J	5.5%	0.000027	0.000070	0.000212	0.011565	0.945907	816.7	±2.9	99.1	10.7	92.2
09G2265K	5.6%	0.000010	0.000035	0.000121	0.006603	0.540735	817.5	±2.9	99.4	6.1	106.0

Table 1 *(continued)*

Run ID	Laser	$^{36}Ar_{air}$	$^{37}Ar_{ca}$	$^{38}Ar_{cl}$	$^{39}Ar_{k}$	$^{40}Ar^{*}$	Age	±2 s	$^{40}Ar^{*}$	$^{39}Ar_{k}$	K/Ca
							(Ma)		(%)	(%)	
Lala deposit											
LLZ-26 (J = 0.0070000 ± 0.0000350)											
09G2265L	5.7%	0.000007	0.000022	0.000104	0.005727	0.468455	816.8	±3.3	99.5	5.3	146.8
09G2265M	5.8%	0.000006	0.000017	0.000126	0.006986	0.571759	817.1	±2.9	99.6	6.5	234.7
09G2265N	6.0%	0.000010	0.000019	0.000138	0.007642	0.626207	817.9	±3.0	99.5	7.1	222.4
09G2265O	6.3%	0.000013	0.000028	0.000212	0.011605	0.951304	818.2	±2.9	99.6	10.7	233.1
09G2265P	6.6%	0.000012	0.000059	0.000317	0.016680	1.369221	819.1	±2.8	99.7	15.4	158.2
09G2265Q	7.5%	0.000004	0.000039	0.000197	0.010760	0.882158	818.2	±2.7	99.8	10.0	154.8
09G2265R	9.0%	0.000003	0.000000	0.000014	0.000829	0.067136	810.4	±10.4	98.9	0.8	154.8
LLZ-27 (J = 0.0070000 ± 0.0000350)											
09G2266B	4.1%	0.000252	0.000007	0.000003	0.000158	0.010473	686.4	±72.2	12.3	0.1	13.0
09G2266C	4.3%	0.000245	0.000029	0.000052	0.002512	0.198507	794.4	±5.6	73.2	1.2	47.9
09G2266D	4.5%	0.000151	0.000014	0.000075	0.003740	0.305159	815.1	±3.8	87.2	1.7	145.0
09G2266E	4.7%	0.000178	0.000019	0.000163	0.008251	0.681106	822.7	±3.0	92.8	3.8	246.5
09G2266F	4.8%	0.000097	0.000017	0.000155	0.008080	0.668147	823.9	±2.9	95.8	3.7	271.6
09G2266H	5.0%	0.000094	0.000021	0.000304	0.016456	1.364238	825.6	±2.8	98.0	7.6	446.1
09G2266I	5.2%	0.000063	0.000025	0.000380	0.020710	1.719368	826.6	±2.8	98.9	9.5	458.1
09G2266J	5.3%	0.000030	0.000026	0.000536	0.029207	2.433030	828.8	±2.8	99.6	13.4	623.2
09G2266K	5.4%	0.000018	0.000024	0.000517	0.027695	2.302793	827.5	±2.7	99.7	12.7	634.1
09G2266L	5.5%	0.000012	0.000024	0.000422	0.022334	1.853123	826.2	±2.8	99.8	10.3	522.1
09G2266M	5.7%	0.000009	0.000027	0.000328	0.017368	1.436880	824.2	±2.8	99.8	8.0	363.9
09G2266N	5.9%	0.000009	0.000032	0.000294	0.015786	1.303262	822.9	±2.9	99.7	7.3	280.1
09G2266O	6.2%	0.000011	0.000043	0.000302	0.016238	1.339082	822.1	±2.7	99.7	7.5	212.8
09G2266P	7.0%	0.000012	0.000043	0.000361	0.018932	1.551559	818.0	±2.8	99.7	8.7	246.2
09G2266Q	9.0%	0.000009	0.000019	0.000195	0.010109	0.823704	814.2	±2.8	99.6	4.7	300.6

and Zhou, 2012). The Re–Os ages demonstrate that the Lala deposit reflects another mineralization event, significantly younger than the Dahongshan and Yinachang deposits. The formation of the Lala deposit at ~1.0 Ga was coeval with eruption of volcanic rocks in the Huili, Julin and Kunyang Groups and the ~1.0 Ga granitic and gabbroic intrusions that intrude rocks of the Huili and Julin Groups (Greentree et al.,

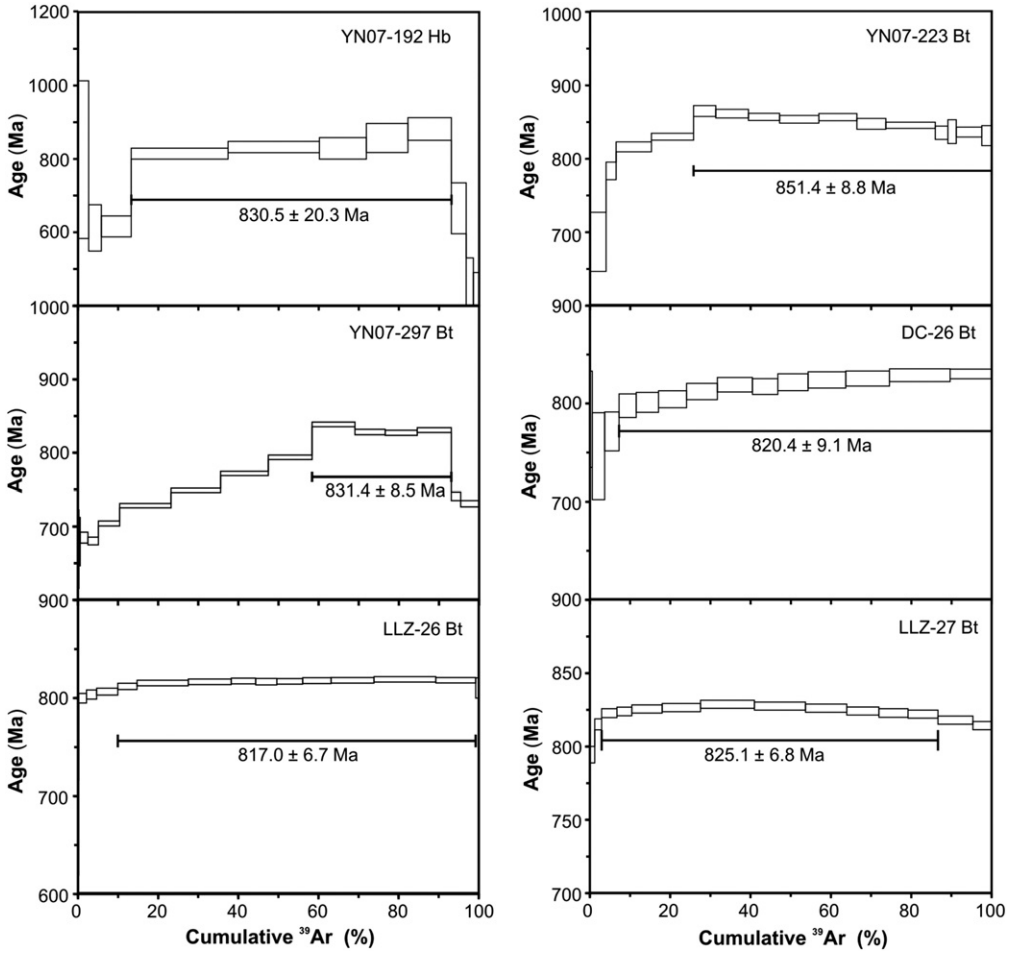

Fig. 17. Laser incremental heating $^{40}Ar/^{39}Ar$ age spectra of biotite and amphibole from the Lala, Yinachang, Xikuangshan, and Dahongshan deposits in the Kangdian metallogenic province.

2006; Geng et al., 2007; Zhang et al., 2007; Chen and Zhou, 2012; Wang et al., 2012a,b; Chen et al., 2014).

There are no precise mineralization ages available for the Sin Quyen deposit. However, the Sin Quyen Group is comparable to the Dongchuan and Dahongshan Groups. In consideration of similar mineralization styles to those hosted in the Dahongshan Group, we suggest that the Sin Quyen deposit likely formed synchronously with the Dahongshan deposit at ~1.66 Ga.

Previous geochronological studies of the Shilu deposit have reported a wide range of ages including an 841 Ma Sm–Nd isochron age of iron ores (Zhang et al., 1992), and a large number of K–Ar and Rb–Sr ages ranging from 590 to 170 Ma (e.g., Chen et al., 2006). Rocks and ores of the Shilu deposit have undergone multiple tectonic events and have been metamorphosed to the amphibolite facies. Thus, these ages could simply reflect resetting of the isotopic system, leaving the true age of mineralization unresolved.

5.2. Neoproterozoic thermal event

Previous studies have reported many K–Ar ages on alteration minerals from some Fe–Cu deposits in the Kangdian province, mostly at ~800 Ma (e.g. Sun et al., 1991a) and $^{40}Ar/^{39}Ar$ ages of quartz associated with ores at 780–870 Ma (Fig. 18) (Ye et al., 2004; Qiu and Jiang, 2007). The present study provides more precise $^{40}Ar/^{39}Ar$ ages of hydrothermal biotite and metamorphic amphibole from several deposits (Fig. 17). These ages are significantly younger than molybdenite Re–Os ages, but are broadly consistent with previous K–Ar and $^{40}Ar/^{39}Ar$ ages. The Re–Os chronometer of molybdenite was probably resistant to late tectonothermal events and high-temperature, hydrothermal activities (e.g. Stein et al., 1998; Selby and Creaser, 2001). However, $^{40}Ar/^{39}Ar$ ages of micas can be easily reset during post-ore thermal events. For example, Selby et al. (2002) obtained Re–Os molybdenite dates identical to the U–Pb zircon age of the host intrusion for lode gold deposits in eastern Alaska, but the hydrothermal and igneous micas have younger $^{40}Ar/^{39}Ar$ ages. These authors suggest that the Re–Os molybdenite method records the timing of sulfide and gold mineralization, whereas the much younger $^{40}Ar/^{39}Ar$ dates reflect post-ore thermal events and/or slow cooling.

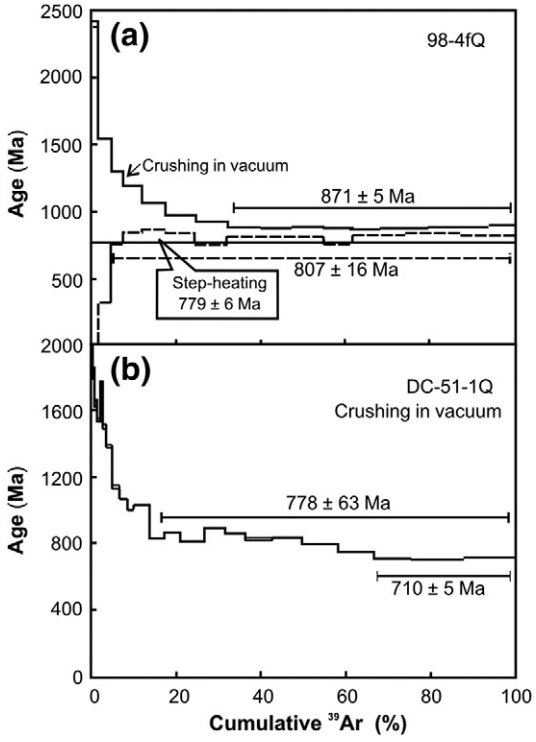

Fig. 18. $^{40}Ar/^{39}Ar$ age spectra of quartz from stratiform (a) and vein-type ores (b), Luoxue mine (Qiu et al., 1998, 2002).

Spatially associated igneous plutons in the province range in age from ~740 to ~860 Ma and include arc granites, adakitic rocks, and subduction-related mafic–ultramafic rocks (Zhou et al., 2002a,b). The $^{40}Ar/^{39}Ar$ ages of hydrothermal minerals from the Fe–Cu deposits are generally compatible with the ages of these Neoproterozoic intrusions in the western Yangtze Block that were metamorphosed to granitic gneisses shortly after their emplacement (He et al., 1988; Deng et al., 2001). We thus suggest that the $^{40}Ar/^{39}Ar$ ages record a post-ore thermal resetting event in the Neoproterozoic, either metamorphic or magmatic (Fig. 19).

5.3. Implications of multiple Fe–Cu mineralization events

The Fe–Cu deposits in the Kangdian province may have formed from multiple mineralization events. Protracted IOCG mineralization involving possible multiple events has been reported for the Cloncurry and Kiruna districts (Smith et al., 2009; Duncan et al., 2011). In both the Cloncurry and Kiruna districts, early IOCG mineralization was associated with regional sodic alteration (Mark et al., 2006; Smith et al., 2009; Duncan et al., 2010, 2011), but the main-stage mineralization took place tens of millions of years later, possibly related to regional metamorphism or magmatism. Local hydrothermal events may have lasted for hundreds of millions years (Duncan et al., 2011). IOCG metallogenic provinces with protracted histories of multiple mineralization events may be a common feature.

6. Fe–Cu mineralization of the Kangdian province and the supercontinental cycles

Formation of some mineral deposits correlates well with the assembly of supercontinents, whereas other deposits may have formed in intra-plate settings during the breakup of supercontinents. Orogenic Au, epithermal Au–Ag, and porphyry Cu ± Au or Mo deposits are characteristic of subduction-related settings (Goldfarb et al., 2010). Both volcanogenic massive sulfide (VMS) deposits and banded iron formations (BIF) formed within extensional zones of convergent margins (Isley and Abbott, 1999; Bekker et al., 2010; Houston et al., 2010). Deposits formed in collisional settings include Mississippi Valley-type (MVT) Pb–Zn deposits, unconformity-type U deposits, and Sn–W deposits (Kerrich et al., 2005; Leach et al., 2010). On the other hand, diamond, Ni–Cu-PGE, IOCG, clastic-dominated (CD) Pb–Zn, and sedimentary-hosted stratiform Cu and some VMS deposits are associated with failed rifting or actual breakup phases of a supercontinent (e.g. Goldfarb et al., 2010; Hitzman et al., 2010 and references therein). The IOCG deposits are genetically related to magmatic–hydrothermal systems in extensional settings, and are spatially associated with A-type granites (e.g. Kerrich et al., 2005; Groves et al., 2010; Elburg et al., 2012). The 2.57 Ga Carajás deposit in Brazil is the oldest known IOCG deposit (Groves et al., 2010). The Paleoproterozoic and Mesoproterozoic IOCG deposits are the most common of this class. Examples include the 1.59 Ga Olympic Dam deposit, Australia, whose formation was related to the breakup of Columbia subsequent to ~2.1 to 1.85 Ga (Zhao et al., 2004; Evans and Mitchell, 2011). The oldest IOCG deposits in the Kangdian province provide more examples of such deposits formed during the breakup of this supercontinent.

6.1. Breakup of Columbia and formation of Fe–Cu deposits

Global-scale 2.1–1.8 Ga continental collision events have been well documented in a number of large continental cratons, and are linked with the assembly of the supercontinent Columbia (Rogers and Santosh, 2002; Zhao et al., 2002, 2004). The Paleoproterozoic tectonic evolution of the Yangtze Block and its position in the reconstructed Columbia supercontinent are still poorly known due to sparse outcrops of

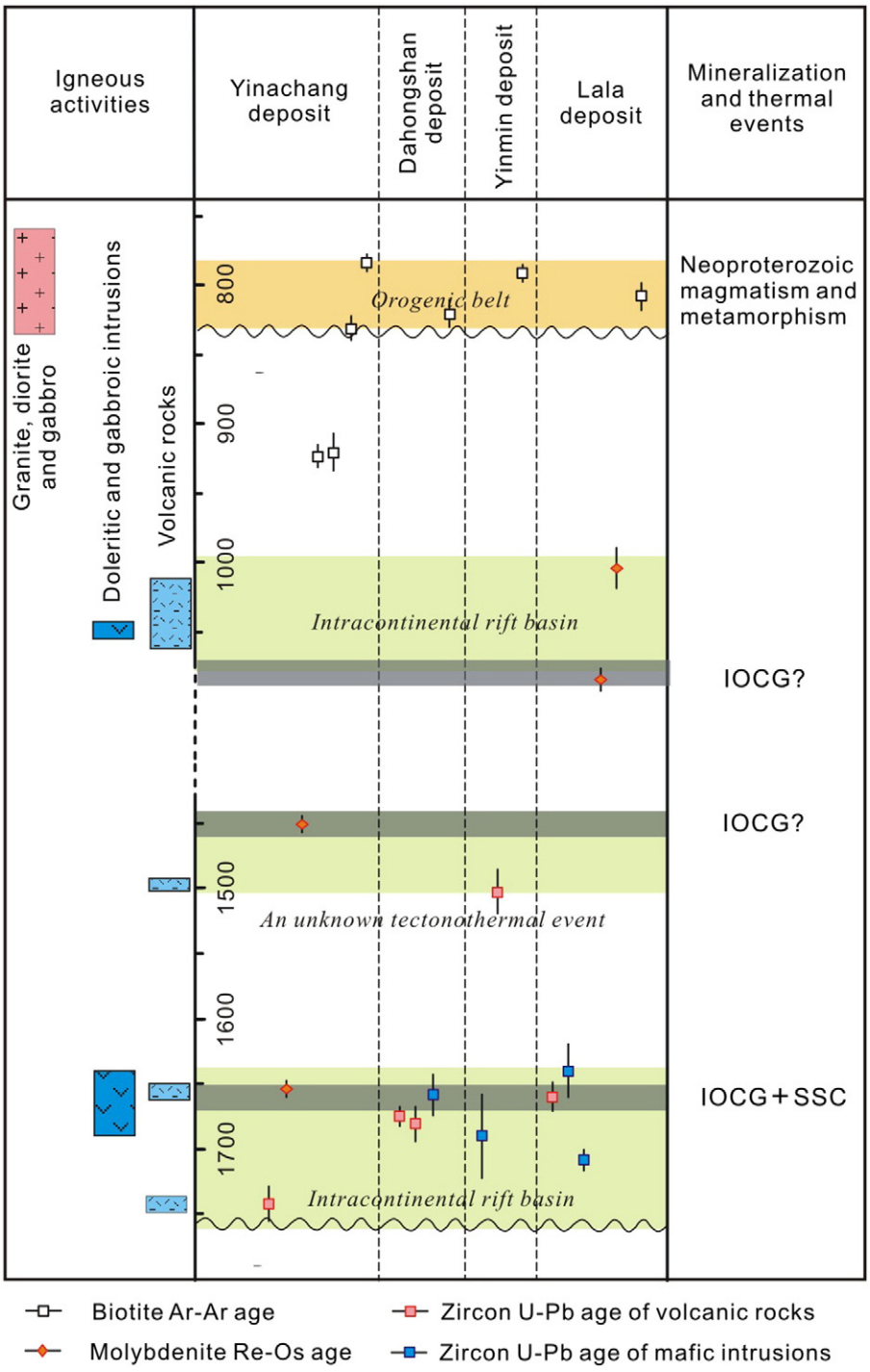

Fig. 19. Summary of geochronological data shows multiple IOCG mineralization events at the Kangdian region and their relationships to regional volcanism, mafic intrusions, and Neoproterozoic tectonothermal events in the Kangdian region. Data sources as referenced in text and includes the data of present study.

Paleoproterozoic rocks. Magmatic and granulite facies metamorphic events at 2.05–1.90 Ga were recently identified in the northern Yangtze Block (Zhang et al., 2006b; Sun et al., 2008; Wu et al., 2008). In the southwestern Yangtze Block, rocks of the Dahongshan, Dongchuan, and Hekou Groups contain 2.05–1.95 Ga detrital zircons with low Th/U ratios, which are also indicative of metamorphism (Zhao et al., 2010; Hieu et al., 2012; W.T. Chen et al., 2013; Z.C. Chen et al., 2013; L. Chen et al., 2013). Therefore, the Yangtze Block has evidence in the assembly of Columbia.

The break-up of Columbia is associated with widespread 1.7–1.3 Ga intra-continental rifting and anorogenic magmatism in many cratons (Condie, 2002; Rogers and Santosh, 2002; Zhao et al., 2002; Ernst et al., 2008; Evans and Mitchell, 2011; Zhang et al., 2012a). In the North China Craton, ~1.70 Ga anorthosite–mangerite–charnockite–rapakivi granite (AMCG) suites and mafic dike swarms have been considered to record the initial fragmentation of Columbia (e.g., Hou et al., 2008; Peng et al., 2008; Zhao et al., 2009). The 1.6–1.4 Ga AMCG suites are also reported in both North America and southern Baltica (Puura and Faloden, 1999; Åhäll et al., 2000). Mafic dikes with ages of 1.59–1.50 Ga in South America are also considered to be associated with such a break-up event (Silveira et al., 2012; Teixeira et al., 2013). The fragmentation of the supercontinent may have continued until its final break-up marked by the emplacement of the ~1.3-Ga Mackenzie dike swarm in North

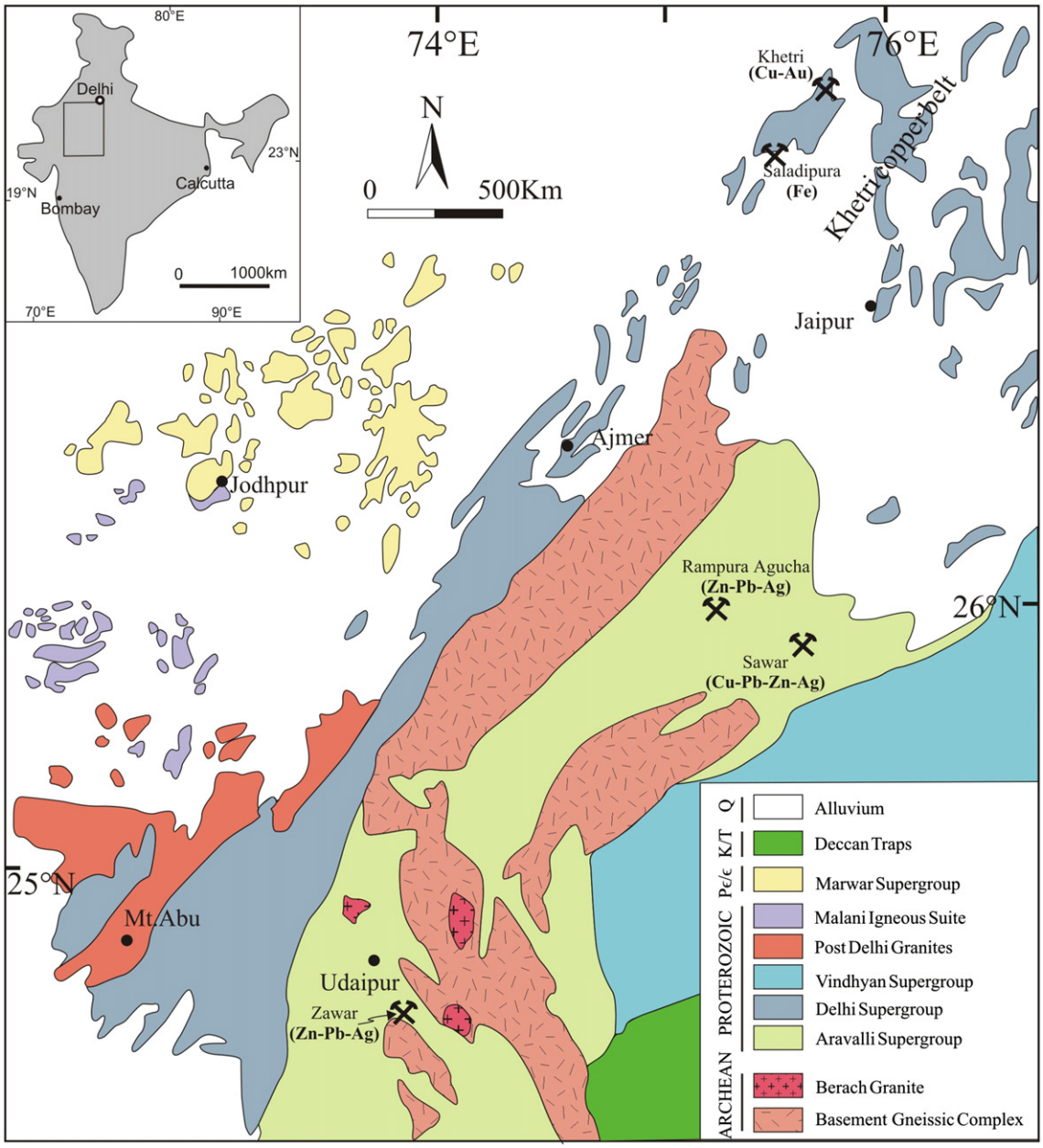

Fig. 20. Simplified geological map of the Aravalli mountain range in NW India, showing the Khetri copper belt in the northernmost (after Knight et al., 2002; Van Lente et al., 2009).

America (Rogers and Santosh, 2002; Evans and Mitchell, 2011). These Mesoproterozoic magmatic events are considered to be mantle-plume related and to have marked the fragmentation of Columbia (Rogers and Santosh, 2002; Zhao et al., 2002, 2004; Hou et al., 2008; Peng et al., 2008; Evans and Mitchell, 2011; Silveira et al., 2012; Teixeira et al., 2013).

Both ~1.8-Ga mafic dikes and rapakivi granites in the northern Yangtze Block are thought to have formed in a continental rifting environment (Peng et al., 2009; Xiong et al., 2009; Zhao et al., 2010; Zhang et al., 2011), possibly related to the initial fragmentation of the Columbia supercontinent. The Dongchuan Group has features indicative of a complete sedimentation from alluvial fan to fluvial system and finally to deep sea basin during the period of 1.7–1.5 Ga (Wang and Zhou, 2014), typical of sedimentation in a continental rifting setting. There are rifting-related ~1.70 to 1.66 Ga bimodal volcanic rocks and associated mafic dikes, suggesting an intra-plate rifting environment at least during the period of ~1.7–1.66 Ga (Zhao et al., 2010; W.T. Chen et al., 2013; Z.C. Chen et al., 2013; L. Chen et al., 2013). Furthermore, Fan et al. (2013) provided the first evidence of mantle plume-related mafic magmatism that produced the ca. 1.5 Ga Fe–Ti–V oxide-bearing intrusions in the northern part of the Kangdian province. The 1.7–1.5 Ga intraplate, continental rift setting in the southwestern Yangtze Block is consistent with widespread 1.6–1.3 Ga Mesoproterozoic post-orogenic and anorogenic magmatism that has been recognized in most Precambrian cratons worldwide. Therefore, the southwestern Yangtze Block underwent intra-plate rifting and mantle plume-related magmatic events during the breakup of Columbia.

Giant IOCG deposits worldwide were formed during the late Paleoproterozoic to early Mesoproterozoic, including world-class deposits in the Cloncurry, Olympic Dam, and Kiruna districts (Hitzman et al., 1992; Hitzman, 2000; Williams et al., 2005; Groves et al., 2010). Groves et al. (2010) suggest that the formation of giant Precambrian IOCG deposits was mainly related to extensive mantle-derived magma underplating the buoyant, metasomatized, subcontinental lithospheric mantle. Some of the IOCG deposits in the Kangdian region could also be related to this global tectonic–metallogenic event, coincident with the break-up of Columbia.

6.2. Linkage of Fe–Cu deposits in SW China, northern Australia, and NW India

On the basis of similar age spectra of detrital zircons and ~1.7 Ga, within-plate magmatism among different blocks in Columbia, the Yangtze Block was considered to possibly link with the North Australian Craton during the Paleoproterozoic (Wang et al., 2012a,b; W.T. Chen et al., 2013; Z.C. Chen et al., 2013; L. Chen et al., 2013). In particular, Paleoproterozoic strata in the Kangdian province are geochemically similar to those of the Leichhardt and Calvert Superbasins, and the Mount Isa Inlier in the North Australian Craton (W.T. Chen et al., 2013; Z.C. Chen et al., 2013; L. Chen et al., 2013). Comparison of rift-related sediments from both continents also argues for such a connection (Wang and Zhou, 2014). In such a scenario, the Yangtze Block could have been positioned in the western part of the Columbia supercontinent as reconstructed by Zhao et al. (2002, 2004).

The linkage of the Yangtze Block with the North Australian Craton is consistent with similar IOCG deposits in these two regions. In the Mount Isa Inlier, several large IOCG deposits include the Ernest Henry, Eloise, Lightning Creek, and Starra in the Cloncurry district (Williams et al., 2005). These deposits have ages of 1.65–1.36 Ga (Duncan et al., 2011), roughly synchronous with the Dahongshan, Xikuangshan and Yinachang deposits in the southwestern Yangtze Block. Moreover, the mineralization styles of the Fe–Cu deposits from the two blocks are comparable. For example, the large Ernest Henry deposit is a breccia-hosted magnetite-dominated deposit, roughly similar to the Xikuangshan deposit.

The Fe–Cu deposits in the Khetri copper belt, northern Aravalli mountain range in NW India have mineralization styles similar to those of Fe–Cu deposits from the Kangdian province. For example, host rocks of the deposits in NW India are the Paleoproterozoic Delhi Supergroup, which comprises shallow-water, locally evaporitic, sedimentary rocks, with lesser mafic and felsic volcanic rocks (Fig. 20) (Knight et al., 2002; Kaur et al., 2013). Such a sedimentary-volcanic succession is comparable to the Dahongshan and Hekou Groups in the southwestern Yangtze Block (Zhao and Zhou, 2011; W.T. Chen et al., 2013; Z.C. Chen et al., 2013; L. Chen et al., 2013). Major Fe–Cu deposits in NW India contain Au, Ag, Co, Fe, REE, and U (Knight et al., 2002). We suggest that these deposits were formed in an intra-continental extensional environment during the breakup of Columbia. Precise ages of Fe–Cu deposits in NW India are not yet available, but Paleoproterozoic strata and Fe–Cu mineralization identical to those in northern Australia and southern China provide evidences for placing them in spatial association as neighbors in Columbia (Fig. 21).

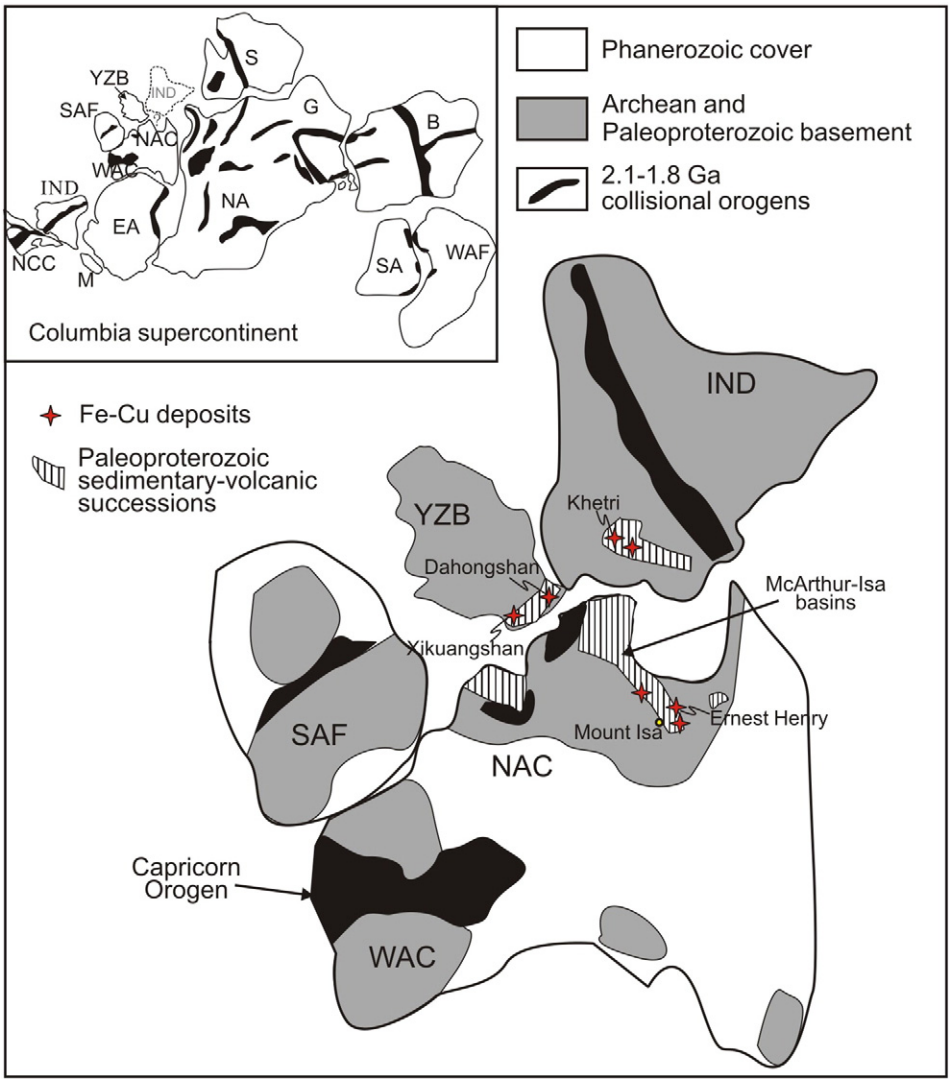

Fig. 21. Possible position of the Yangtze Block in the Columbia supercontinent reconstructed by Zhao et al. (2002). Abbreviations: B — Baltica; EA — East Antarctica; G — Greenland; IND — India; M — Madagascar; NA — North America; NAC — North Australian Craton; NCC — North China Craton; SAF — South Africa; SA — South America; S — Siberia; WAF — West Africa; WAC — West Australian Craton; YZB — Yangtze Block.

6.3. Post-Columbia tectonic evolution and Fe–Cu mineralization

It has been thought that South China was part of the Rodinia supercontinent, partly on the basis of major Grenvillian orogenic belts in the Yangtze Block (Li et al., 1995, 2003c). Such orogenic belts were taken as evidence for a correlation between South China, Australia, and Laurentia (Li et al., 2003c). According to Li et al. (1995), South China was located in an intracratonic setting between eastern Australia and western Laurentia. It has been further suggested that the Neoproterozoic igneous rocks of the Yangtze Block are products of a mantle plume, marking the pre-breakup of Rodinia and subsequent migration of the Yangtze Block (Li et al., 1995, 2003c). However, recent studies do not support the existence of Grenvillian orogenic belts in South China (Zhao et al., 2011). The Neoproterozoic mantle plume model is inconsistent with the lack of voluminous basaltic rocks or the absence of mafic dike swarms, komatiites, and picrites, which are commonly associated with plume activity.

After the breakup of Columbia, the western Yangtze Block became a passive continental margin in which rocks of the ~1.0 Ga Huili, Julin and Kunyang Groups were deposited unconformably above those of the Dongchuan, Hekou, and Dahongshan Groups. These strata contain considerable amounts of volcanic rocks. The igneous event also produced gabbroic intrusions with SHRIMP zircon U–Pb ages of ~1.0 Ga (Greentree et al., 2006; Geng et al., 2007; Zhang et al., 2007; and our unpublished data). These rocks were previously interpreted as part of a Grenvillian orogen in South China (Li et al., 2002, 2008), but they have geochemical affinities of intraplate igneous rocks (Greentree et al., 2006; Geng et al., 2007; Zhang et al., 2007; Chen et al., 2014). The anorogenic features of the ~1.0-Ga magmatism in the southwestern Yangtze Block again do not support Grenvillian orogenic activity in the Yangtze Block. The Yangtze Block may have been in a passive margin setting during the assembly of the supercontinent Rodinia (Chen et al., 2014). We thus tentatively suggest that the ~1.05 Ga Lala deposit and possibly some other deposits of the Kangdian IOCG province may have formed in an intraplate extensional environment (Chen and Zhou, 2012).

Extensive arc-related magmatism between 860 and 740 Ma in the western Yangtze Block is supportive of a long-term subduction system. During this period, sedimentation was generally waning except for the ~860 Ma Yanbian Group which was deposited in a back-arc basin (Sun et al., 2008). Oceanic subduction under the southwestern Yangtze Block likely stopped at ~740 Ma and was followed by deposition of the Cryogenian 725–630 Ma glacial-interglacial sedimentary sequences in a passive margin, marking a major regional unconformity.

Rocks of the Neoproterozoic Bikou Group were recently identified as products of sedimentation in a fore-arc basin sequence (Yan et al., 2004), supporting the subduction model (Sun et al., 2009). In contrast to the model proposed by Li et al. (1995, 2003c), the South China Block, including the Yangtze Block, has been linked by other workers to northwestern Australia in the Neoproterozoic (Zhou et al., 2002a,b; Yu et al., 2008; Wang and Zhou, 2012). It is possible that in the configuration of Rodinia, South China may have been attached to Madagascar, the Seychelles Islands, and Malani in India, all being placed northwest of Australia (Wang and Zhou, 2012), a significantly different position compared to that proposed by Li et al. (1995, 2003c).

The Aravalli mountain range in NW India has Neoproterozoic igneous rocks and strata (e.g., Malani and Sirohi Groups) similar to the Kangdian province. We envisage that the North Australian Craton was separated from the other two blocks during the breakup of Columbia. In the Rodinia supercontinent, both the southwestern Yangtze Block and NW Indian Block were still together but in a subduction-related environment, thus marginal to the supercontinent. They were probably separated after the breakup of Rodinia and joined the assembly of Gondwanaland separately.

7. Conclusions

The Fe–Cu deposits in the Kangdian IOCG province formed in multiple mineralization events mainly at 1.65 Ga and ~1.0 Ga. A less important, local hydrothermal event probably also occurred at 1.45 Ga. Hydrothermal minerals have $^{40}Ar/^{39}Ar$ ages clustering at 870–780 Ma, significantly younger than the mineralization events, but contemporaneous with the major Neoproterozoic magmatic event in the southwestern Yangtze Block. Both the Shilu and Sin Quyen deposits may have undergone additional Mesozoic–Cenozoic tectonothermal overprints. The occurrences of these deposits support the linkage of South China, India, and Australia in the reconstruction of supercontinent Columbia. India and South China were separated during the breakup of Rodinia.

Acknowledgments

This study was supported by the National Natural Science Foundation of China (41272212), Research Grant Council of Hong Kong (17306814) and the CAS/SAFEA International Partnership Program for Creative Research Teams–Intraplate Mineralization Research Team (KZZDEW-TZ-20). We thank local geologists from mines, particular the Sin Quyen Cu mine and Shilu Fe mine for guiding us with field work and anonymous reviewers for providing constructive comments.

References

Åhäll, K.I., Connelly, J.N., Brewer, T.S., 2000. Episodic rapakivi magmatism due to distal orogenesis?: correlation of 1.69–1.50 Ga orogenic and inboard "anorogenic" events in the Baltic shield. Geology 28, 823–826.
Bekker, A., Slack, J.F., Planavsky, N., Krapež, B., Hofmann, A., Konhauser, K.O., Rouxel, O.J., 2010. Iron formations: the sedimentary product of a complex interplay among mantle, tectonic, oceanic, and biosphere processes. Econ. Geol. 105, 467–508.
Cai, J.-X., Zhang, K.-J., 2009. A new model for the Indochina and South China collision during the Late Permian to the Middle Triassic. Tectonophysics 467, 35–43.
Cawood, P.A., Hawkesworth, C.J., 2013. Temporal relations between mineral deposits and global tectonic cycles: implications for prospectivity. In: Jenkins, G. (Ed.), Ore Deposits and Earth HistoryGeol. Soc. Lond. Spec. Publ. 393. http://dx.doi.org/10.1144/SP393.1.
Chen, H., Ran, C., 1992. Isotope Geochemistry of Copper Deposits in Kangdian Axis. Geological Publishing House, Beijing, p. 100 (in Chinese with English abstract).
Chen, W.T., Zhou, M.F., 2012. Paragenesis, stable isotopes and molybdenite Re–Os isotopic age of the Lala iron copper deposit, Southwest China. Econ. Geol. 107, 459–480.
Chen, X.Y., Wang, Y.J., Fan, W.M., Peng, T.P., Ge, T.H., 2006. Microstructure characteristics of NE trend ductile shear zones of southwestern Hainan: constraints from ^{40}Ar–^{39}Ar geochronology. Geochimica 35, 479–488.
Chen, H.Y., Clark, A.H., Kyser, T.K., Ullrich, T.D., Baxter, R., Chen, Y.M., Moody, T.C., 2010. Evolution of the giant Marcona–Mina Justa iron oxide–copper–gold district, South-Central Peru. Econ. Geol. 105, 155–185.
Chen, W.T., Zhou, M.F., Zhao, X.F., 2013a. Late Paleoproterozoic sedimentary and mafic rocks in the Hekou area, SW China: implication for the reconstruction of the Yangtze Block in Columbia. Precambrian Res. 231, 61–77.
Chen, Z.C., Lin, W., Faure, M., Lepvrier, C., Chu, Y., Wang, Q.C., 2013b. Geochronological constraint of early Mesozoic tectonic event at Northeast Vietnam. Acta Petrol. Sin. 29, 1825–1840.
Chen, L., Zhang, Z., Song, H., 2013c. Weak depth and along-strike variations in stretching from a multi-episodic finite stretching model: evidence for uniform pure-shear extension in the opening of the South China Sea. J. Asian Earth Sci. 78, 358–370.
Chen, W.T., Sun, W.H., Wang, W., Zhao, J.H., Zhou, M.F., 2014. "Grenvillian" intra-plate mafic magmatism in the southwestern Yangtze Block, SW China. Precambrian Res. 242, 138–153.
Condie, K.C., 2002. Breakup of a Paleoproterozoic supercontinent. Gondwana Res. 5, 41–43.
Cui, Y.L., 2008. Metallogeny and Prospecting Implications of the Longbohe Cu Deposit, Jinping, Yunnan Province. Publishing House of Science and Technology of Yunnan, p. 233, (in Chinese).
Deng, S.X., Wang, J.H., Zhu, B.Q., 2001. P–T–t path of metamorphism for the Julin Group and its geodynamical implications in Yuanmou, Yunnan. Sci. China Ser. D Earth Sci. 44, 609–620.
Duncan, R., Hitzman, M., Nelson, E., Stein, H., Zimmerman, A., Kirwin, D., 2010. Re–Os molybdenite ages for the southern Cloncurry IOCG district, Queensland, Australia: protracted mineralisation over 210 myr. Smart Science for Exploration and Mining vols. 1 and 2. James Cook University, Townsville, pp. 626–628.
Duncan, R.J., Stein, H.J., Evans, K.A., Hitzman, M.W., Nelson, E.P., Kirwin, D.J., 2011. A new geochronological framework for mineralization and alteration in the Selwyn–Mount Dore Corridor, Eastern Fold Belt, Mount Isa Inlier, Australia: genetic implications for iron oxide copper–gold deposits. Econ. Geol. 106, 169–192.
Elburg, M., Anderson, T., Bons, P.D., Weisheit, A., Simonsen, S.L., Smet, I., 2012. Metasomatism and metallogeny of A-type granites of the Mt. Painter–Mt Babbage Inliers, South Australia. Lithos 151, 83–104.

Ernst, R.E., Wingate, M.T.D., Buchan, K.L., Li, Z.X., 2008. Global record of 1600–700 Ma Large Igneous Provinces (LIPs): implications for the reconstruction of the proposed Nuna (Columbia) and Rodinia supercontinents. Precambrian Res. 160, 159–178.
Evans, D.A.D., Mitchell, R.N., 2011. Assembly and breakup of the core of Paleoproterozoic–Mesoproterozoic supercontinent Nuna. Geology 39, 443–446.
Fan, H.-P., Zhu, Wei-Guang, Li, Zheng-Xiang, Zhong, Hong, Bai, Zhong-Jie, He, De-Feng, Chen, Cai-Jie, Cao, Chong-Yong, 2013. Ca. 1.5 Ga mafic magmatism in South China during the break-up of the supercontinent Nuna/Columbia: the Zhuqing Fe–Ti–V oxide ore-bearing mafic intrusions in western Yangtze Block. Lithos 168–169, 85–98.
Gao, S., Yang, J., Zhou, L., Li, M., Hu, Z., Guo, J., Yuan, H., Gong, H., Xiao, G., Wei, J., 2011. Age and growth of the Archean Kongling terrain, South China, with emphasis on 3.3 Ga granitoid gneisses. Am. J. Sci. 311, 153–182.
Gas'kov, I.V., Anh, T.T., Hoa, T.T., Dung, P.T., Nevol'ko, P.A., Can, P.N., 2012. The Sin Quyen Cu–Fe–Au-REE deposit (northern Vietnam): composition and formation conditions. Russ. Geol. Geophys. 53, 442–456.
Geng, Y., Yang, C., Du, L., Wang, X., Ren, L., Zhou, X., 2007. Chronology and tectonic environment of the Tianbaoshan Formation: new evidence from zircon SHRIMP U–Pb age and geochemistry. Geol. Rev. 53, 556–563 (in Chinese with English abstract).
Geng, Y., Liu, Y., Gao, L., Peng, N., Jiang, X., 2012. Geochronology of the Mesoproterozoic Tongan Formation in Southwestern margin of Yangtze Craton: new evidence from zircon LA-ICPMS U–Pb ages. Acta Geol. Sin. 86, 1479–1490 (in Chinese with English abstract).
Goldfarb, R.J., Bradley, D., Leach, D.L., 2010. Secular variation in economic geology. Econ. Geol. 105, 459–465.
Gong, L., He, Y., Chen, T., 1996. Proterozoic Dongchuan-type Rift Cu Deposit in Yunnan. Metallurgical Industry Publication, Beijing, p. 248 (in Chinese with English abstract).
Greentree, M.R., Li, Z.X., 2008. The oldest known rocks in south-western China: SHRIMP U–Pb magmatic crystallisation age and detrital provenance analysis of the Paleoproterozoic Dahongshan Group. J. Asian Earth Sci. 33, 289–302.
Greentree, M.R., Li, Z.X., Li, X.H., Wu, H., 2006. Late Mesoproterozoic to earliest Neoproterozoic basin record of the Sibao orogenesis in western South China and relationship to the assembly of Rodinia. Precambrian Res. 151, 79–100.
Groves, D.I., Bierlein, F.P., Meinert, L.D., Hitzman, M.W., 2010. Iron Oxide Copper–Gold (IOCG) deposits through Earth history: implications for origin, lithospheric setting, and distinction from other epigenetic iron oxide deposits. Econ. Geol. 105, 641–654.
Gu, L.X., Khin, Z., Hu, W.X., Zhang, K.J., Ni, P., He, J.X., Xu, Y.T., Lu, J.J., Lin, C.M., 2007. Distinctive features of Late Palaeozoic massive sulphide deposits in South China. Ore Geol. Rev. 31, 107–138.
He, J., Chen, G., Yang, Z., Min, J., Liu, X., 1988. The Kangdian Grey Gneisses. Chongqing Publishing House, Chongqing, p. 174 (in Chinese with English abstract).
Hieu, P.T., Chen, F., Me, L.T., Thuy, N.T.B., Siebel, W., Lan, T.-G., 2012. Zircon U–Pb ages and Hf isotopic compositions from the Sin Quyen Formation: the Precambrian crustal evolution of northwest Vietnam. Int. Geol. Rev. 54, 1548–1561.
Hitzman, M.W., 2000. Iron oxide–Cu–Au deposits: what, where, when, and why. In: Porter, T.M. (Ed.), Hydrothermal Iron Copper Gold & Related Deposits: A Global Perspective vol. 1. PGC Publishing, Adelaide, Australia, pp. 9–25.
Hitzman, M.W., Oreskes, N., Einaudi, M.T., 1992. Geological characteristics and tectonic setting of Proterozoic iron oxide (Cu–U–Au-REE) deposits. Precambrian Res. 58, 241–287.
Hitzman, M.W., Selley, D., Bull, S., 2010. Formation of sedimentary rock-hosted copper deposits through Earth history. Econ. Geol. 105, 627–639.
Hou, G., Santosh, M., Qian, X., Lister, G.S., Li, J., 2008. Configuration of the Late Paleoproterozoic supercontinent Columbia: insights from radiating mafic dyke swarms. Gondwana Res. 14, 395–409.
Houston, D.L., Pehrsson, S., Eglington, B.M., Zaw, K., 2010. The geology and metallogeny of volcanic-hosted massive sulfide deposits: variations through geologic time and with tectonic setting. Econ. Geol. 105, 571–591.
Hu, A., Zhu, B., Mao, C.U., Zhu, N., Hunang, R., 1991. Geochronology of the Dahongshan Group. Chin. J. Geochem. 10, 195–203.
Isley, A.E., Abbott, D.H., 1999. Plume-related mafic volcanism and the deposition of banded iron formations. J. Geophys. Res. 104, 15461–15477.
Kaur, P., Zeh, A., Chaudhri, N., Gerdes, A., Okrusch, M., 2013. Nature of magmatism and sedimentation at a Columbia active margin: insights from combined U–Pb and Lu–Hf isotope data of detrital zircons from NW India. Gondwana Res. 23, 1040–1052.
Kerrich, R., Goldfarb, R.J., Richards, J.P., 2005. Metallogenic provinces in an evolving geodynamic framework. Econ. Geol. 100th Anniv. Vol. 1097–1136.
Knight, J., Joy, S., Lowe, J., Cameron, J., Merrillees, J., Nag, S., Shah, N., Dua, G., Jhala, K., 2002. The Khetri copper belt, Rajasthan: iron oxide copper–gold terrane in the Proterozoic of NW India. In: Porter, T.M. (Ed.), Hydrothermal Iron Oxide Copper–Gold & Related Deposits: A Global Perspective vol. 2. PGC Publishing, Adelaide, pp. 321–341.
Koppers, A.A.P., 2002. ArArCALC—software for $^{40}Ar/^{39}Ar$ age calculations. Comput. Geosci. 28, 605–619.
Leach, D.L., Bradley, D.C., Huston, D., Pisarevsky, S.A., Taylor, R.D., Gardoll, S.J., 2010. Sediment-hosted lead zinc deposits in Earth history. Econ. Geol. 105, 593–625.
Li, Z.X., Zhang, L., Powell, C.M., 1995. South China in Rodinia: part of the missing link between Australia–East Antarctica and Laurentia. Geology 23, 410–707.
Li, X.H., Li, Z.X., Zhou, H.W., Liu, Y., Kinny, P.D., 2002. U–Pb zircon geochronology, geochemistry and Nd isotopic study of Neoproterozoic bimodal volcanic rocks in the Kangdian Rift of South China: implications for the initial rifting of Rodinia. Precambrian Res. 113, 135–154.
Li, X.H., Li, Z.X., Ge, W., Zhou, H., Li, W., Liu, Y., Wingate, M.T.D., 2003a. Neoproterozoic granitoids in South China: crustal melting above a mantle plume at ca. 825 Ma? Precambrian Res. 122, 45–83.
Li, Z.Q., Wang, J.Z., Liu, J.J., Li, C.Y., Du, A.D., Liu, Y.P., Ye, L., 2003b. Re–Os dating of molydenite from Lala Fe-Oxide–Cu–Au–Mo-REE deposit, Southwest China: implications for ore genesis. Contrib. Geol. Miner. Resour. Res. 18, 39–42 (in Chinese with English abstract).
Li, Z.X., Li, X.H., Kinny, P.D., Wang, J., Zhang, S., Zhou, H., 2003c. Geochronology of Neoproterozoic syn-rift magmatism in the Yangtze Craton, South China and correlations with other continents: evidence for a mantle superplume that broke up Rodinia. Precambrian Res. 122, 8–109.
Li, X.H., Li, Z.X., Li, W.X., Wang, Y.J., 2006. Initiation of the Indosinian Orogeny in South China: evidence for a Permian magmatic arc on Hainan Island. J. Geol. 114, 34–353.
Li, Z.X., Bogdanovab, S.V., Collins, A.S., Davidson, A., Waele, B., Ernste, R.E., Fitzsimons, I.C. W., Fuck, R.A., Gladkochub, D.P., Jacobs, J., Karlstrom, K.E., Lu, S., Natapov, L.M., Pease, V., Pisarevsky, S.A., Thrane, K., Vernikovskyp, V., 2008. Assembly, configuration, and break-up history of Rodinia: a synthesis. Precambrian Res. 160, 179–210.
Li, X.H., Li, W.X., Li, Z.X., Lo, C.H., Wang, J., Ye, M.F., Yang, Y.H., 2009. Amalgamation between the Yangtze and Cathaysia Blocks in South China: constraints from SHRIMP U–Pb zircon ages, geochemistry and Nd–Hf isotopes of the Shuangxiwu volcanic rocks. Precambrian Res. 174, 117–128.
Liu, H.L., Zheng, H.B., Wang, Y.L., Lin, Q.J., Wu, C.H., Zhao, M.S., Du, Y.K., 2011. Basement of the South China area: tracing the Tethyan realm. Acta Geol. Sin. 85, 637–655.
Mark, G., Oliver, N.H.S., Carew, M.J., 2006. Insights into the genesis and diversity of epigenetic Cu–Au mineralisation in the Cloncurry district, Mt Isa Inlier, northwest Queensland. Aust. J. Earth Sci. 53, 109–124.
Mclean, R.N., 2002. The Sin Quyen iron oxide–copper–gold-rare earth oxide mineralization of North Vietnam. In: Porter, T.M. (Ed.), Hydrothermal Iron Oxide Copper–Gold & Related Deposits: A Global Perspective 2. PGC Publishing, Adelaide, pp. 293–301.
NGTYP, (Nonferrous Geological Team 313 of Yunnan Province), 2006. Synthesized geological report of the Dahongshan deposit, Xinping County, Yunnan Province. Unpublished report.
Peng, P., Zhai, M.-G., Ernst, R., Guo, J.-H., Liu, F., Hu, B., 2008. A 1.78 Ga Large Igneous Province in the North China craton: the Xiong'er Volcanic Province and the North China dyke swarm. Lithos 101, 260–280.
Peng, M., Wu, Y.B., Wang, J., Jiao, W.F., Liu, X.C., Yang, S.H., 2009. Paleoproterozoic mafic dyke from Kongling terrain in the Yangtze Craton and its implication. Chin. Sci. Bull. 54, 1098–1104.
Puura, V., Faloden, T., 1999. Rapakivi–granite–anorthosite magmatism: a way of thinning and stabilization of the Svecofennian crust, Baltic, Sea basin. Tectonophysics 305, 75–92.
Qian, J., Shen, Y., 1990. The Dahongshan Volcanogenic Fe–Cu Deposit in Yunnan Province. Geological Publishing House, Beijing, p. 236 (in Chinese with English abstract).
Qiu, H.N., Sun, D.D., Zhu, B.Q., Chang, X.Y., 1998. $^{40}Ar/^{39}Ar$ dating for quartz samples from the Dongchuan copper deposit, Yunnan, by crushing in vacuum and by incremental heating on its powder. Geochemia 27, 335–343.
Qiu, H.N., Jiang, Y.D., 2007. Sphalerite $^{40}Ar/^{39}Ar$ progressive crushing and stepwise heating techniques. Earth Planet. Sci. Lett. 256, 224–232.
Qiu, H.N., Zhu, B.Q., Sun, D.H., 2002. Age significance interpreted from $^{40}Ar/^{39}Ar$ dating of quartz samples from the Dongchuan copper deposits, Yunnan, SW China, by crushing and heating. Geochem. J. 36, 475–491 (in Chinese with English Abstract).
Replumaz, A., Tapponnier, P., 2003. Reconstruction of the deformed collision zone between India and Asia by backward motion of lithospheric blocks. J. Geophys. Res. 108 (B6), 2285 (1–24).
Rogers, J.J.W., Santosh, M., 2002. Configuration of Columbia, a Mesoproterozoic supercontinent. Gondwana Res. 5, 5–22.
SBGMR (Sichuan Bureau of Geology and Mineral Resources), 1991. Regional Geology of Sichuan Province. Geological Publishing House, Beijing.
Selby, D., Creaser, R.A., 2001. Re–Os geochronology and systematics in molybdenite from the Endako Porphyry molybdenum deposit, British Columbia, Canada. Econ. Geol. 96, 197–204.
Selby, D., Creaser, R.A., Hart, C.J.R., Rombach, C.S., Thompson, J.F.H., Smith, M.T., Bakke, A.A., Goldfarb, R.J., 2002. Absolute timing of sulfide and gold mineralization: a comparison of Re–Os molybdenite and Ar–Ar mica methods from the Tintina Gold Belt, Alaska. Geology 30, 791–794.
Shu, L.-S., Zhou, G.-Q., Shi, Y.-S., Yin, J., 1993. Study of high pressure metamorphic blueschist and its late Proterozoic age in the eastern Jiangnan belt. Chin. Sci. Bull. 20, 1879–1882.
Silveira, E.M., Söderlund, U., Oliveira, E.P., Ernst, R.E., Menezes Leal, A.B., 2012. First precise U–Pb baddeleyite ages of 1500 Ma mafic dykes from the São Francisco Craton, Brazil, and tectonic implications. Lithos 174, 144–156.
Smith, M.P., Storey, C.D., Jeffries, T.E., Ryan, C., 2009. In situ U–Pb and trace element analysis of accessory minerals in the Kiruna District, Norrbotten, Sweden: new constraints on the timing and origin of mineralization. J. Petrol. 50, 2063–2094.
Steiger, R.H., Jäger, E., 1977. Subcommission on geochronology: convention on the use of decay constants in geo- and cosmochronology. Earth Planet. Sci. Lett. 36, 359–362.
Stein, H.J., Markey, R.J., Morgan, J.W., Sundblad, K., Motuza, G., 1998. Re–Os ages for Archean molybdenite and pyrite, Kuittila–Kivisuo, Finland and Proterozoic molybdenite, Kabeliai, Lithuania: testing the chronometer in a metamorphic and metasomatic setting. Mineral. Deposita 33, 329–345.
Sun, K., Shen, Y., Liu, G., Li, Z., Pan, X., 1991a. Proterozoic Iron–Copper Deposits in Central Yunnan Province. China University of Geoscience Press, Wuhan, p. 169 (in Chinese with English abstract).
Sun, K., Shen, Y., Liu, G., Li, Z., Pan, X., 1991b. Dianzhong Proterozoic Iron–Copper Deposits. China University of Geoscience Press, Wuhan, p. 169 (in Chinese with English abstract).
Sun, W.H., Zhou, M.F., Zhao, J.H., 2007. Geochemistry and tectonic significance of basaltic lavas in the Neoproterozoic Yanbian Group (Southern Sichuan Province, SW China). Int. Geol. Rev. 49, 554–571.
Sun, W.H., Zhou, M.F., Yan, D.P., Li, J.W., Ma, Y.X., 2008. Provenance and tectonic setting of the Neoproterozoic Yanbian Group, western Yangtze Block (SW China). Precambrian Res. 167, 213–236.

Sun, Z.M., Yin, F.G., Guan, J.L., Liu, J.H., Li, J.M., Geng, Y.R., Wang, L.Q., 2009. SHRIMP U–Pb dating and its stratigraphic significance of tuff zircons from Heishan Formation of Kunyang Group, Dongchuan area, Yunnan Province, China. Geol. Bull. China 28, 896–900 (in Chinese with English abstract).
Tapponnier, P., Lacassin, R., Leloup, P.H., Scharer, U., Dalai, Z., Haiwei, W., Xiaohan, L., Shaocheng, J., Lianshang, Z., Jiayou, Z., 1990. The Ailao Shan/Red River metamorphic belt: tertiary left-lateral shear between Indochina and South China. Nature 343, 431–437.
Teixeira, W., D'Agrella-Filho, M.S., Hamilton, M.A., Ernst, R.E., Girardi, V.A.V., Mazzucchelli, M., Bettencourt, J.S., 2013. U–Pb (ID-TIMS) baddeleyite ages and paleomagnetism of 1.79 and 1.59 Ga tholeiitic dyke swarms, and position of the Rio de la Plata Craton within the Columbia supercontinent. Lithos 174, 157–174.
Van Lente, B., Ashwal, L.D., Pandit, M.K., Bowring, S.A., Torsvik, T.H., 2009. Neoproterozoic hydrothermally altered basaltic rocks from Rajasthan, northwest India: implications for late Precambrian tectonic evolution of the Aravalli Craton. Precambrian Res. 170, 202–222.
Wang, Y.Z., Ding, J., 1996. Structural deformation and evolution of the medium to high grade metamorphic rocks series in the Ailao Mountains, Yunnan. Tethyan Geol. 20, 52–69 (in Chinese with English abstract).
Wang, W., Zhou, M.-F., 2012. Sedimentary records of the Yangtze Block (South China) and their correlation with equivalent Neoproterozoic sequences on adjacent continents. Sediment. Geol. 265–266, 126–142.
Wang, W., Zhou, M.-F., 2014. Provenance and tectonic setting of the Paleo- to Mesoproterozoic Dongchuan Group in the southwestern Yangtze Block, South China: implication for the breakup of the supercontinent Columbia. Tectonophysics 610, 110–127.
Wang, X.F., Ma, D.Q., Jiang, D.H. (Eds.), 1991. Geology of Hainan Island: The 1st, Stratum and Paleo-biology. Geology Publishing House, Beijing, pp. 7–32 (In Chinese).
Wang, W., Wang, F., Chen, F., Zhu, X., Xiao, P., Siebel, W., 2010. Detrital zircon ages and Hf-Nd isotopic composition of Neoproterozoic sedimentary rocks in the Yangtze Block: constraints on the deposition age and provenance. J. Geol. 118, 79–94.
Wang, L.J., Yu, J.H., Griffin, W.L., O'Reilly, S.Y., 2012a. Early crustal evolution in the western Yangtze Block: evidence from U–Pb and Lu–Hf isotopes on detrital zircons from sedimentary rocks. Precambrian Res. 222–223, 368–385.
Wang, Z., Zhou, B., Guo, Y., Yang, B., Liao, Z., Wang, S., 2012b. Geochemistry and zircon U–Pb dating of Tangtang granite in the western margin of the Yangtze Platform. Acta Petrol. Mineral. 31, 652–662.
Wang, W., Zhou, M.F., Yan, D.P., Li, L., Malpas, J., 2013. Detrital zircon record of Neoproterozoic active-margin sedimentation in the eastern Jiangnan Orogen, South China. Precambrian Res. 235, 1–19.
Weihed, P., Arndt, N., Billström, K., Duchesne, J.-C., Eilu, P., Martinsson, O., Papunen, H., Lahtinen, R., 2005. Precambrian geodynamics and ore formation: the Fennoscandian Shield. Ore Geol. Rev. 2, 273–322.
Williams, P.J., Barton, M.D., Johnson, D.A., Fontbote, L., Haller De, A., Mark, G., Oliver, N.H.S. , Marschik, R., 2005. Iron oxide copper–gold deposits: geology, space–time distribution, and possible modes of origin. Econ. Geol. 100th Anniv. Vol. 371–405.
Wu, M.D., Duan, J.S., Song, X.L., Chen, L., Dan, Y., 1990. Geology of Kunyang Group in Yunnan Province. Scientific Press of Yunnan Province, Kunming, p. 265 (in Chinese with English abstract).
Wu, Y.B., Zheng, Y.F., Gao, S., Jiao, W.F., Liu, Y.S., 2008. Zircon U–Pb age and trace element evidence for Paleoproterozoic granulite-facies metamorphism and Archean crustal rocks in the Dabie Orogen. Lithos 101, 308–322.
Xiong, Q., Zheng, J.P., Yu, C.M., Su, Y.P., Tang, H.Y., Zhang, Z.H., 2009. Zircon U–Pb age and Hf isotope of Quanyishang A-type granite in Yichang: signification for the Yangtze continental cratonization in Paleoproterozoic. Chin. Sci. Bull. 54, 436–446.
Xu, D.R., Xia, B., Li, P.C., Chen, G.H., Ma, C., Zhang, Y.Q., 2007. Protolith natures and U–Pb sensitive high mass-resolution ion microprobe (SHRIMP) zircon ages of the metabasites in Hainan Island, South China: implications for geodynamic evolutions since the late Precambrian. Island Arc 16, 575–597.
Xu, D.R., Xiao, Y., Xia, B., Cai, R.J., Hou, W., Wang, L., Liu, Z.L., Zhao, B., 2009. Metallogenic Model and Ore Predicating of the Shilu Iron Ore Deposit in Hainan Province. China. Geology Publishing House, Beijing, p. 331 (in Chinese).
Xu, D.R., Wang, Z.L., Cai, J.X., Wu, C.J., Bakun-Czubarow, N., Wang, L., Chen, H.Y., Baker, M.J., Kusia, M.A., 2013. Geological characteristics and metallogenesis of the Shilu Fe-ore deposit in Hainan Province, South China. Ore Geol. Rev. 53, 318–342.
Yan, Q., Hanson, A.D., Wang, Z.Q., Druschke, A.P., Yan, Z., Wang, T., Liu, D., Song, B., Jian, P., Zhou, H., Jiang, C., 2004. Neoproterozoic subduction and rifting on the northern margin of the Yangtze Plate, China: implications for Rodinia reconstruction. Int. Geol. Rev. 46, 817–832.
YBGMR (Yunnan Bureau of Geology and Mineral Resources), 1990. Regional Geology of Yunnan Province. Geological Publishing House, Beijing.
Ye, L., Li, C.Y., Liu, J.J., Liu, Y.P., 2004. Ar–Ar isotopic age Yinachang copper deposit, Wuding, Yunnan Province, China and its implications. Acta Mineral. Sin. 24, 411–414 (in Chinese with English abstract).
Yu, J.H., O'Reilly, S.Y., Wang, L., Griffin, W.L., Zhang, M., Wang, R., Jiang, S., Shu, L., 2008. Where was South China in the Rodinia supercontinent?: evidence from U–Pb geochronology and Hf isotopes of detrital zircons. Precambrian Res. 164, 1–15.
Yumul Jr., G.P., Zhou, M.F., Wang, C.Y., Zhao, T.P., Dimalanta, C.B., 2007. Geology and geochemistry of the Shuanggou ophiolite (Ailaoshan ophiolitic belt), Yunnan Province, SW China: evidence for a slow-spreading oceanic basin origin. J. Asian Earth Sci. 32, 385–395.
Zhai, M.G., Cong, B.L., Qiao, G.S., Zhang, R.Y., 1990. Sm–Nd and Rb–Sr geochronology of metamorphic rocks from SW Yunnan orogenic zones, China. Acta Petrol. Sin. 4, 1–11 (in Chinese with English abstract).
Zhang, R.J., Ma, G.G., Jiang, D.H., 1990. Precambrian Geology of Hainan Island, South China. Geology Publishing House, Beijing, p. 130 (in Chinese with English abstract).
Zhang, R.J., Ma, G.G., Hong, S.N., Yan, D.P., 1992. The Sm–Nd isotopic age of Shilu iron ores in Hainan Island and its implications. Sci. Geol. Sin. 21, 38–43 (in Chinese with English Abstract).
Zhang, Y.M., Zhang, R.J., Rao, H.Z., Ma, G.G., 1997. The Precambrian crustal tectonic evolution in Hainan Island. Earth Sci. 22, 395–400 (in Chinese with English Abstract).
Zhang, S.B., Zheng, Y.F., Wu, Y.B., Zhao, Z.F., Gao, S., Wu, F.Y., 2006a. Zircon U–Pb age and Hf isotope evidence for 3.8 Ga crustal remnant and episodic reworking of Archean crust in South China. Earth Planet. Sci. Lett. 252 (1–2), 56–71.
Zhang, S.B., Zheng, Y.F., Wu, Y.B., Zhao, Z.F., Gao, S., Wu, F.Y., 2006b. Zircon U–Pb age and Hf–O isotope evidence for Paleoproterozoic metamorphic event in South China. Precambrian Res. 151, 265–288.
Zhang, C.H., Gao, L.Z., Wu, Z.J., Shi, X.Y., Yan, Q.R., Li, D.J., 2007. SHRIMP U–Pb zircon age of tuff from the Kunyang group in central Yunnan: evidence for Grenvillian orogeny in south China. Chin. Sci. Bull. 52, 1517–1525.
Zhang, L.J., Ma, C.Q., Wang, L.X., She, Z.B., Wang, S.M., 2011. Discovery of Paleoproterozoic rapakivi granite on the northern margin of the Yangtze Block and its geological significance. Chin. Sci. Bull. 56, 306–318.
Zhang, S., Li, Z.X., Evans, D.A.D., Wu, H., Li, H., 2012a. Pre-Rodinia supercontinent Nuna shaping up: a global synthesis with new paleomagnetic results from North China. Earth Planet. Sci. Lett. 353–354, 145–155.
Zhang, S.B., Wu, R.X., Zheng, Y.F., 2012b. Neoproterozoic continental accretion in South China: geochemical evidence from the Fuchuan ophiolite in the Jiangnan orogen. Precambrian Res. 220–221, 45–64.
Zhao, X.-F., 2010. Paleoproterozoic crustal evolution and Fe-Cu metallogeny of the western Yangtze block, Unpublished Ph.D. thesis, University of Hong Kong, SW China, p. 192.
Zhao, J.H., Zhou, M.F., 2007. Geochemistry of Neoproterozoic mafic intrusions in the Panzhihua district (Sichuan Province, SW China): implications for subduction-related metasomatism in the upper mantle. Precambrian Res. 152, 27–47.
Zhao, J.H., Zhou, M.F., 2008. Neoproterozoic adakitic plutons in the northern margin of the Yangtze Block, China: partial melting of a thickened lower crust and implications for secular crustal evolution. Lithos 104, 231–248.
Zhao, X.F., Zhou, M.F., 2011. Fe–Cu deposits in the Kangdian region, SW China: a Proterozoic IOCG (iron-oxide–copper–gold) metallogenic province. Mineral. Deposita 46, 731–747.
Zhao, G., Cawood, P.A., Wilde, S.A., Sun, M., 2002. Review of global 2.1–1.8 Ga orogens: implications for a pre-Rodinia supercontinent. Earth Sci. Rev. 59, 125–162.
Zhao, G., Sun, M., Wilde, S.A., Li, S., 2004. A Paleo-Mesoproterozoic supercontinent: assembly, growth and breakup. Earth Sci. Rev. 67, 91–123.
Zhao, T.P., Chen, W., Zhou, M.F., 2009. Geochemical and Nd–Hf isotopic constraints on the origin of the ~1.74-Ga Damiao anorthosite complex, North China Craton. Lithos 113, 673–690.
Zhao, X.F., Zhou, M.F., Li, J.W., Sun, M., Gao, J.F., Sun, W.H., Yang, J.H., 2010. Late Paleoproterozoic to early Mesoproterozoic Dongchuan Group in Yunnan, SW China: implications for tectonic evolution of the Yangtze Block. Precambrian Res. 182, 57–69.
Zhao, J.H., Zhou, M.F., Yan, D.P., Zheng, J.P., Li, J.W., 2011. Reappraisal of the ages of Neoproterozoic strata in South China: no connection with the Grenvillian orogeny. Geology 39, 299–302.
Zhao, X.F., Zhou, M.F., Hitzman, M.W., Li, J.W., Bennett, M., Meighan, C., Anderson, E., 2012. Late Paleoproterozoic to Early Mesoproterozoic Tangdan sedimentary rock-hosted strata-bound copper deposit, Yunnan Province, Southwest China. Econ. Geol. 107, 357–375.
Zhao, X.F., Zhou, M.F., Li, J.W., Selby, D., Li, X.H., Qi, L., 2013. Sulfide Re–Os and Rb–Sr isotopic dating of the Kangdian IOCG metallogenic province, SW China: implications for regional metallogenesis. Econ. Geol. 108, 1489–1498.
Zheng, J.P., Griffin, W.L., O'Reilly, S.Y., Zhang, M., Pearson, N., Pan, Y., 2006. Widespread Archean basement beneath the Yangtze Craton. Geology 34, 417–420.
Zhou, M.F., Kennedy, A.K., Sun, M., Malpas, J., Lesher, C.M., 2002a. Neoproterozoic arc-related mafic intrusions along the northern margin of South China: implications for the accretion of Rodinia. J. Geol. 110, 611–618.
Zhou, M.F., Yan, D.P., Kennedy, A.K., Li, Y., Ding, J., 2002b. SHRIMP U–Pb zircon geochronological and geochemical evidence for Neoproterozoic arc-magmatism along the western margin of the Yangtze Block, South China. Earth Planet. Sci. Lett. 196, 51–67.
Zhou, M.F., Ma, Y., Yan, D.P., Xia, X., Zhao, J.H., Sun, M., 2006. The Yanbian Terrane (Southern Sichuan Province, SW China): a Neoproterozoic arc assemblage in the western margin of the Yangtze Block. Precambrian Res. 144, 19–38.
Zhou, D., Sun, Z., Chen, H.Z., Xu, H.H., Wang, W.Y., Pang, X., Cai, D.S., Hu, D.K., 2008. Mesozoic paleogeography and tectonic evolution of South China Sea and adjacent areas in the context of Tethyan and Paleo-Pacific interconnections. Island Arc 17, 186–207.
Zhou, J.C., Wang, X.L., Qiu, J.S., 2009. Geochronology of Neoproterozoic mafic rocks and sandstones from northeastern Guizhou, South China: coeval arc magmatism and sedimentation. Precambrian Res. 170, 27–42.
Zhu, Z.M., Zeng, L.X., Zhou, J.Y., Luo, L.P., Chen, J.B., Shen, B., 2009. Lala iron oxide–copper–gold deposit in Sichuan Province: evidence from mineralography. Geol. J. China Univ. 15, 485–495 (in Chinese with English abstract).